

A Small-Molecule Screen Identifies L-Kynurenine as a Competitive Inhibitor of TAA1/TAR Activity in Ethylene-Directed Auxin Biosynthesis and Root Growth in *Arabidopsis*

Wenrong He,^a Javier Brumos,^b Hongjiang Li,^{a,c} Yusi Ji,^a Meng Ke,^d Xinqi Gong,^d Qinglong Zeng,^a Wenyang Li,^a Xinyan Zhang,^a Fengying An,^a Xing Wen,^a Pengpeng Li,^a Jinfang Chu,^e Xiaohong Sun,^e Cunyu Yan,^e Nieng Yan,^d De-Yu Xie,^f Natasha Raikhel,^c Zhenbiao Yang,^c Anna N. Stepanova,^b Jose M. Alonso,^b and Hongwei Guo^{a,1}

^a State Key Laboratory of Protein and Plant Gene Research, College of Life Sciences, Peking University, Peking-Tsinghua Center for Life Sciences, Beijing 100871, China

^b Department of Genetics, North Carolina State University, Raleigh, North Carolina 27695

^c Center for Plant Cell Biology, Department of Botany and Plant Sciences, University of California, Riverside, California 92507

^d Center for Structural Biology, School of Life Sciences, Tsinghua University, Beijing 100084, China

^e National Center for Plant Gene Research, Institute of Genetics and Developmental Biology, Chinese Academy of Sciences, Beijing 100101, China

^f Department of Plant Biology, North Carolina State University, Raleigh, North Carolina 27695

The interactions between phytohormones are crucial for plants to adapt to complex environmental changes. One example is the ethylene-regulated local auxin biosynthesis in roots, which partly contributes to ethylene-directed root development and gravitropism. Using a chemical biology approach, we identified a small molecule, L-kynurenine (Kyn), which effectively inhibited ethylene responses in *Arabidopsis thaliana* root tissues. Kyn application repressed nuclear accumulation of the ETHYLENE INSENSITIVE3 (EIN3) transcription factor. Moreover, Kyn application decreased ethylene-induced auxin biosynthesis in roots, and TRYPTOPHAN AMINOTRANSFERASE OF ARABIDOPSIS1/TRYPTOPHAN AMINOTRANSFERASE RELATEDs (TAA1/TARs), the key enzymes in the indole-3-pyruvic acid pathway of auxin biosynthesis, were identified as the molecular targets of Kyn. Further biochemical and phenotypic analyses revealed that Kyn, being an alternate substrate, competitively inhibits TAA1/TAR activity, and Kyn treatment mimicked the loss of TAA1/TAR functions. Molecular modeling and sequence alignments suggested that Kyn effectively and selectively binds to the substrate pocket of TAA1/TAR proteins but not those of other families of aminotransferases. To elucidate the destabilizing effect of Kyn on EIN3, we further found that auxin enhanced EIN3 nuclear accumulation in an EIN3 BINDING F-BOX PROTEIN1 (EBF1)/EBF2-dependent manner, suggesting the existence of a positive feedback loop between auxin biosynthesis and ethylene signaling. Thus, our study not only reveals a new level of interactions between ethylene and auxin pathways but also offers an efficient method to explore and exploit TAA1/TAR-dependent auxin biosynthesis.

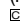
INTRODUCTION

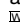
Ethylene is a simple gaseous hormone that regulates many processes in plant growth and development, such as seed germination, cell elongation, fruit ripening, leaf senescence, and resistance to pathogen invasion and stress (reviewed in Johnson and Ecker, 1998; Bleecker and Kende, 2000). Several ethylene response mutants have been identified based on observation of the triple response phenotype, namely, shortened

and thickened roots and hypocotyls, as well as exaggerated hook curvature in the presence of ethylene or its synthetic precursor 1-aminocyclopropane-1-carboxylic acid (ACC). Genetic and molecular biology studies on these mutants have led to the establishment of a largely linear ethylene signaling pathway from receptors in the endoplasmic reticulum membrane to transcription factors in the nucleus. Binding of ethylene gas to the receptors inactivates CONSTITUTIVE TRIPLE RESPONSE1 (CTR1), a Raf-like kinase that acts as a negative regulator of ethylene signaling (Kieber et al., 1993). CTR1 blocks downstream ethylene signaling events by reducing the protein level of ETHYLENE-INSENSITIVE2 (EIN2), an endoplasmic reticulum-associated membrane protein functioning as an essential positive regulator of ethylene signaling (Alonso et al., 1999). In the nucleus, EIN3 and EIN3 LIKE1 (EIL1) are two primary transcription factors operating genetically downstream of EIN2 (Chao et al., 1997; An et al., 2010). Two F-box proteins, EIN3 BINDING

¹ Address correspondence to hongweig@pku.edu.cn.

The author responsible for distribution of materials integral to the findings presented in this article in accordance with the policy described in the Instructions for Authors (www.plantcell.org) is: Hongwei Guo (hongweig@pku.edu.cn).

 Some figures in this article are displayed in color online but in black and white in the print edition.

 Online version contains Web-only data.

www.plantcell.org/cgi/doi/10.1105/tpc.111.089029

F-BOX PROTEIN1 (EBF1) and EBF2, are responsible for the degradation of EIN3 and EIL1 and maintain the minimal level of EIN3 and EIL1 proteins in the absence of ethylene (Guo and Ecker, 2003; Potuschak et al., 2003; Gagne et al., 2004). Upon ethylene application, the levels of EBF1 and EBF2 are down-regulated by a yet unknown mechanism (An et al., 2010), so that the accumulated EIN3 and EIL1 proteins activate the expression of many ethylene response genes.

The interactions among phytohormones are crucial for plants to adapt to complex environmental changes. Auxin is another vital hormone regulating a wide array of processes throughout the plant life span (reviewed in Benjamins and Scheres, 2008). Interestingly, many mutants showing tissue-specific, especially root-specific, ethylene-insensitive phenotypes were found to have defects in auxin transport or biosynthesis, including *auxin-resistant1* (Bennett et al., 1996), *ethylene-insensitive root1/pin-formed2* (*eir1/pin2*) (Luschnig et al., 1998; Müller et al., 1998), and *weak ethylene insensitive2* (*wei2*), *wei7*, and *wei8* (Stepanova et al., 2005, 2008). *AUX1* and *EIR1/PIN2* encode different auxin transporters (Bennett et al., 1996; Luschnig et al., 1998; Müller et al., 1998), whereas the three *WEI* genes encode distinct enzymes in local auxin biosynthesis (Stepanova et al., 2005, 2008). Characterization of these mutants suggests that ethylene-regulated local auxin biosynthesis and distribution is an important mechanism underlying the short-root phenotype of the ethylene triple response (Stepanova et al., 2005, 2007, 2008; Růžická et al., 2007; Swarup et al., 2007).

WEI2 and *WEI7* encode the α - and β -subunits, respectively, of anthranilate synthase, a key enzyme in Trp biosynthesis (Stepanova et al., 2005). Trp is a common precursor of multiple auxin biosynthesis pathways. The findings that ethylene upregulates the expression levels of *WEI2* and *WEI7* and that *wei2* and *wei7* loss-of-function mutants are partially insensitive to ethylene in a root elongation assay suggest a key role for *WEI2/7*-mediated Trp biosynthesis in ethylene-induced root inhibition (Stepanova et al., 2005). More direct evidence came from the identification of *WEI8/SAV3/TIR2* (Stepanova et al., 2008; Tao et al., 2008; Yamada et al., 2009), a gene whose expression is also notably induced by ethylene in roots. *WEI8* encodes TRYPTOPHAN AMINOTRANSFERASE OF ARABIDOPSIS1 (TAA1), the key enzyme catalyzing the conversion of Trp to indole-3-pyruvic acid (IPyA) in one of the auxin biosynthesis pathways (the IPyA pathway) (Stepanova et al., 2008; Tao et al., 2008). Two TAA1 homologs, TRYPTOPHAN AMINOTRANSFERASE RELATED1 (TAR1) and TAR2, were also found to participate in the IPyA pathway (Stepanova et al., 2008). Several recent studies elucidated the crucial roles of TAA1 and the IPyA pathway in plant developmental processes, such as shade avoidance responses (Tao et al., 2008), root development (Stepanova et al., 2008; Yamada et al., 2009), and root gravitropism (Yamada et al., 2009) of *Arabidopsis thaliana* as well as vegetative and reproductive development of maize (*Zea mays*; Phillips et al., 2011).

Although accumulating evidence began to highlight its importance, the auxin biosynthesis pathway has remained elusive compared with auxin polar transport or signal transduction pathways. Auxin research has been greatly advanced by the use of many auxin analogs, antagonists, and transport inhibitors (reviewed in De Rybel et al., 2009a). In fact, most of the key

players in auxin response pathways (metabolism, transport, and signaling) have been identified in genetic screens using these auxin-like molecules or inhibitors. Unlike the large repertoire of small molecules closely linked with auxin perception or transport, few compounds have been reported that specifically act on auxin biosynthesis (reviewed in De Rybel et al., 2009a). Although several small molecules were identified to be potential inhibitors of Trp and/or indole-3-acetic acid (IAA) biosynthesis (Tsurusaki et al., 1990; Koshiba et al., 1993; Ilić et al., 1999; Ludwig-Müller et al., 2010), none of their biological functions, target proteins, and/or modes of action have been well characterized. Recently, a genomics-based approach identified aminoethoxyvinylglycine (AVG) and L-aminoethoxyvinylglycine as inhibitors of auxin biosynthesis, probably by inhibiting Trp aminotransferase (Soeno et al., 2010). However, these inhibitors are nonspecific, as they are likely to affect all or most pyridoxal-5'-phosphate (PLP)-dependent enzymes, such as ACC synthases (ACSs) in ethylene biosynthesis (Huai et al., 2001). In fact, AVG has been widely used as an inhibitor of ACS (Boller et al., 1979). The lack of specific inhibitors of auxin biosynthesis imposes an obstacle to the pharmacological study of auxin production and its action mode.

Chemical genetics is a powerful approach that has the potential to overcome the genetic redundancy and lethality problems frequently encountered in classical forward genetics (reviewed in Crews and Splittgerber, 1999). Given its unique advantages, chemical genetics has begun to gain attention and has been increasingly used in plant signal transduction research, leading to the identification of many new analogs, agonists, and inhibitors of plant hormone pathways, particularly in auxin, abscisic acid (ABA), and brassinosteroid responses (Armstrong et al., 2004; De Rybel et al., 2009b; Park et al., 2009). In this study, we isolated a small molecule, L-kynurenine (Kyn), as a potent inhibitor of ethylene responses in *Arabidopsis* roots and identified its target proteins, TAA1/TARs, a class of key enzymes in the IPyA pathway of auxin biosynthesis. We found that Kyn, as an alternate substrate of TAA1/TARs, competitively and selectively inhibits the TAA1/TAR family but not other related aminotransferases. Furthermore, using Kyn to manipulate TAA1-dependent auxin biosynthesis, we uncovered a positive feedback loop between auxin biosynthesis and ethylene signaling pathways, in which IAA accelerates its own synthesis in roots at least partly by indirectly stabilizing EIN3 protein.

RESULTS

Identification of Kyn, a Small Molecule Leading to Ethylene Insensitivity in *Arabidopsis* Root Tissues

To identify downstream factors of the ethylene signaling pathway, a chemical genetics approach was used to screen a chemical library (SP 2000, <http://www.msdiscovery.com>) in search for suppressors of the constitutive ethylene response phenotypes of *ethylene overproducer1-2* (*eto1-2*) (Wang et al., 2004) or *ctr1-1*. The 3-d-old etiolated seedlings of the two mutants exhibited a typical triple response phenotype, including shortened hypocotyls and roots, as well as exaggerated hook bending (Figure 1A).

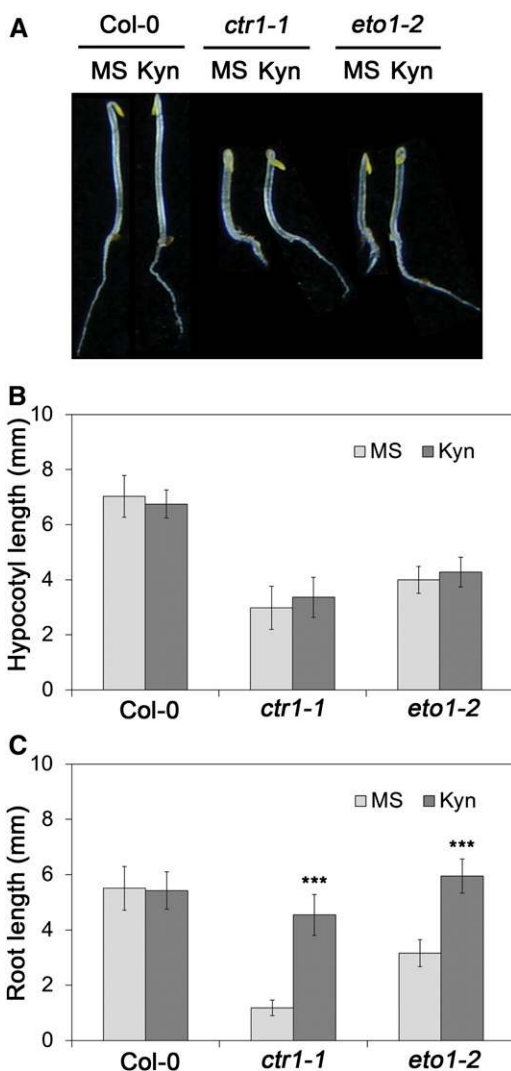


Figure 1. Low Concentrations of Kyn Suppress Root-Specific Phenotypes of *ctr1-1* and *eto1-2*.

(A) Three-day-old etiolated seedlings of Col-0, *ctr1-1*, and *eto1-2* grown on MS medium or MS medium supplemented with 1 μ M Kyn.

(B) and **(C)** Quantification of the hypocotyl lengths **(B)** and root lengths **(C)** of seedlings shown in **(A)**. Bars represent the average length (\pm SD) of at least 20 seedlings (Student's *t* test, between Kyn-treated and non-treated seedlings; ****P* < 0.001).

[See online article for color version of this figure.]

Approximately 10 etiolated seedlings were germinated for 3 d in each well of 96-well microplates containing one of the selected 2000 diverse chemicals at a concentration of 50 to 100 μ M. After two rounds of screening, Kyn was identified as a potent root-specific ethylene response suppressor, as it dramatically reversed the short-root phenotype of *eto1-2* and *ctr1-1* etiolated seedlings (Figures 1A and 1C) but had little effect on hypocotyl length and apical hook curvature at the concentrations initially used (Figures 1A and 1B). As little as 0.01 μ M Kyn was able to promote root elongation of *ctr1-1*, and 0.5 μ M Kyn seemed to reach the maximal

root-promoting effect (see Supplemental Figure 1 online). We further found that Kyn application reversed the root growth inhibitory effect of exogenous ACC treatment on etiolated wild-type seedlings (Figure 2A). In addition to promoting root elongation in the presence of activated ethylene signaling, Kyn treatment also effectively suppressed ACC-induced root hair formation (see Supplemental Figure 2A online). Moreover, when treated with high concentrations of Kyn, such as 30 μ M or higher, the hooks of 3-d-old Columbia-0 (Col-0), *ctr1-1*, and *eto1-2* etiolated seedlings started to open (see Supplemental Figure 3 online), indicating the requirement of higher doses of Kyn to suppress ethylene responses in aerial tissues. Therefore, we identified a small compound, Kyn, which effectively and preferentially suppresses ethylene-induced root growth inhibition and root hair development.

Kyn Represses the Activity and Nuclear Accumulation of EIN3 in Roots

The evident suppression of the *ctr1-1* root phenotype suggested that Kyn affects a cellular event downstream of CTR1. To determine further how Kyn influences the ethylene signaling pathway, we examined the effect of Kyn on *EIN3ox*, a transgenic plant constitutively overexpressing *EIN3* and showing a typical triple response phenotype (Chao et al., 1997; An et al., 2010). Kyn effectively increased the root length of *EIN3ox* in the absence of exogenous ethylene treatment (Figure 2A). However, upon ACC treatment, *EIN3ox* displayed an extremely short root, and simultaneous Kyn application only partially suppressed this severe root inhibition (Figure 2A). This result indicated an antagonistic effect of Kyn on *EIN3* function, implying that Kyn could modulate the activity of *EIN3* or other signaling molecules acting downstream of *EIN3*.

We then investigated whether Kyn application influences the function of *EIN3*. A transgenic reporter line that harbors the β -glucuronidase (*GUS*) gene driven by five tandem repeats of the *EIN3* binding site (EBS) followed by the minimal 35S promoter, *EBS:GUS*, has been previously used to monitor the transcriptional activity of *EIN3* (Stepanova et al., 2007). We found that Kyn inhibited *GUS* activity primarily in root tips of both *ctr1 EBS:GUS* and Col *EBS:GUS* treated with ACC (Figure 2B). Consistent with the aforementioned observations on the severity of the root phenotype, Kyn also reduced the *GUS* expression in the root tips of *EIN3ox* grown in the absence of ACC. Upon ACC treatment, *GUS* staining became overly intensified and extended from the root tips to upper regions of the roots (Figure 2B), indicative of excessively high levels of *EIN3* activity under this condition. Not surprisingly, Kyn application consistently but only modestly repressed the *GUS* staining of *EIN3ox* in the presence of ACC. Moreover, in agreement with its root-specific effect, a low concentration of Kyn (1.5 μ M) failed to abrogate the ACC-induced *GUS* expression in hypocotyls and cotyledons (see Supplemental Figure 2B online). These results clearly indicate that *EIN3*, the core transcription factor of the ethylene signaling pathway, is functionally repressed by Kyn application in roots. Supporting this notion, Kyn had no further effect on either root elongation or *GUS* staining in the *ein2* or *ein3 eil1* mutant backgrounds (see Supplemental Figures 4A and 4B online).

Since the regulation of *EIN3* protein accumulation is a principal mechanism of controlling its function, we next asked whether

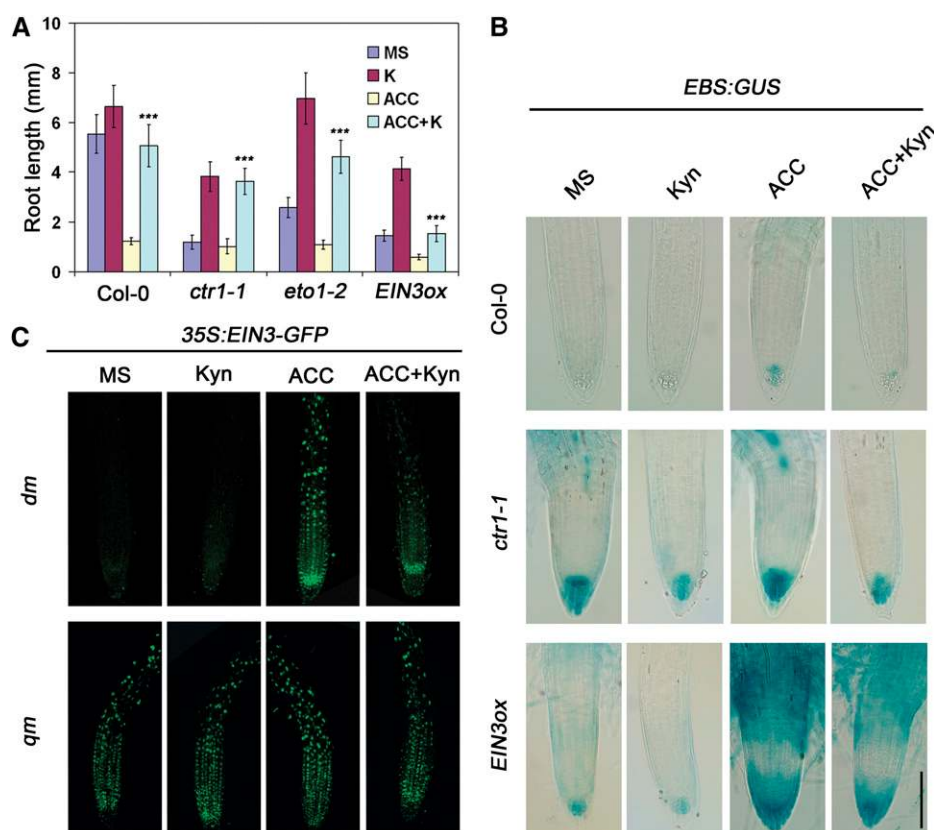


Figure 2. Kyn Inhibits EIN3 Nuclear Accumulation in Roots.

(A) Quantification of the root lengths of 3-d-old etiolated Col-0, *ctr1-1*, *eto1-2*, and *EIN3ox* (an EIN3-overexpressing transgenic line) seedlings grown on MS medium supplemented with 10 μ M ACC and/or 1.5 μ M Kyn (K). The bars represent the average length (\pm SD) of at least 20 seedlings (Student's *t* test, between ACC and ACC+Kyn treatment; ****P* < 0.001).

(B) GUS staining of *EBS:GUS* in the roots of Col-0, *ctr1-1*, and *EIN3ox*. The seedlings were grown on MS medium supplemented with 10 μ M ACC and/or 1.5 μ M Kyn. Bar = 100 μ m.

(C) GFP fluorescence of *35S:EIN3-GFP* in the roots of *ein3 eil1* double (*dm*) and *ein3 eil1 ebf1 ebf2* quadruple (*qm*) mutants. The seedlings were grown on MS medium in the dark for 3 d and then transferred into liquid MS medium supplemented with 100 μ M ACC and/or 100 μ M Kyn and incubated in dark for 3 to 4 h.

Kyn regulates EIN3 accumulation. Two types of transgenic plants were used toward this end: a complemented *ein3 eil1* double mutant (*dm*) harboring *35S:EIN3-GFP* (for green fluorescent protein) that shows normal ethylene response and an *ein3 eil1 ebf1 ebf2* quadruple mutant (*qm*) harboring *35S:EIN3-GFP* that shows constitutive EIN3 accumulation and is completely insensitive to ethylene treatment (An et al., 2010) (Figure 3A). We found that, in the double mutant, ACC treatment strongly stabilized the EIN3-GFP protein in the nuclei of root tips and elongation zones, and Kyn application noticeably reversed this effect (Figure 2C). By contrast, Kyn did not affect the constitutive EIN3-GFP nuclear accumulation in the *qm* background (Figure 2C), suggesting that Kyn inhibits EIN3 protein accumulation likely by promoting EBF1/EBF2-mediated EIN3 degradation.

Kyn Negatively Regulates Auxin Responses

Interestingly, in the *ein3 eil1 ebf1 ebf2 35S:EIN3-GFP* line, in which EIN3-GFP level was not affected by the Kyn treatment, we can still

observe a weak but appreciable effect of Kyn on augmenting root elongation (Figures 3A and 3B). This observation led us to speculate that this effect results from Kyn-mediated regulation of additional components downstream of EIN3. Several earlier studies have demonstrated that ethylene inhibits root growth by modulating auxin biosynthesis and transport (Stepanova et al., 2005, 2007, 2008; Růžička et al., 2007; Swarup et al., 2007). Therefore, we suspected that Kyn might also function in the regulation of auxin response. We first monitored auxin signaling activity using a *DR5:GUS* reporter line and found that Kyn reduced the GUS expression in the root tips (Figure 3C). The decrease of GUS staining was much more pronounced when ethylene signaling was activated by ACC treatment or in *ctr1*. Conversely, in ethylene-insensitive mutants, such as *ein2* or *ein3 eil1*, the *DR5:GUS* expression was quite low and the Kyn-mediated effect was negligible (Figure 3C). These results support the idea that the ethylene-induced auxin response is repressed by Kyn treatment. Furthermore, the constitutive low basal levels and the marginal effect of Kyn treatment on the *DR5:GUS* expression in

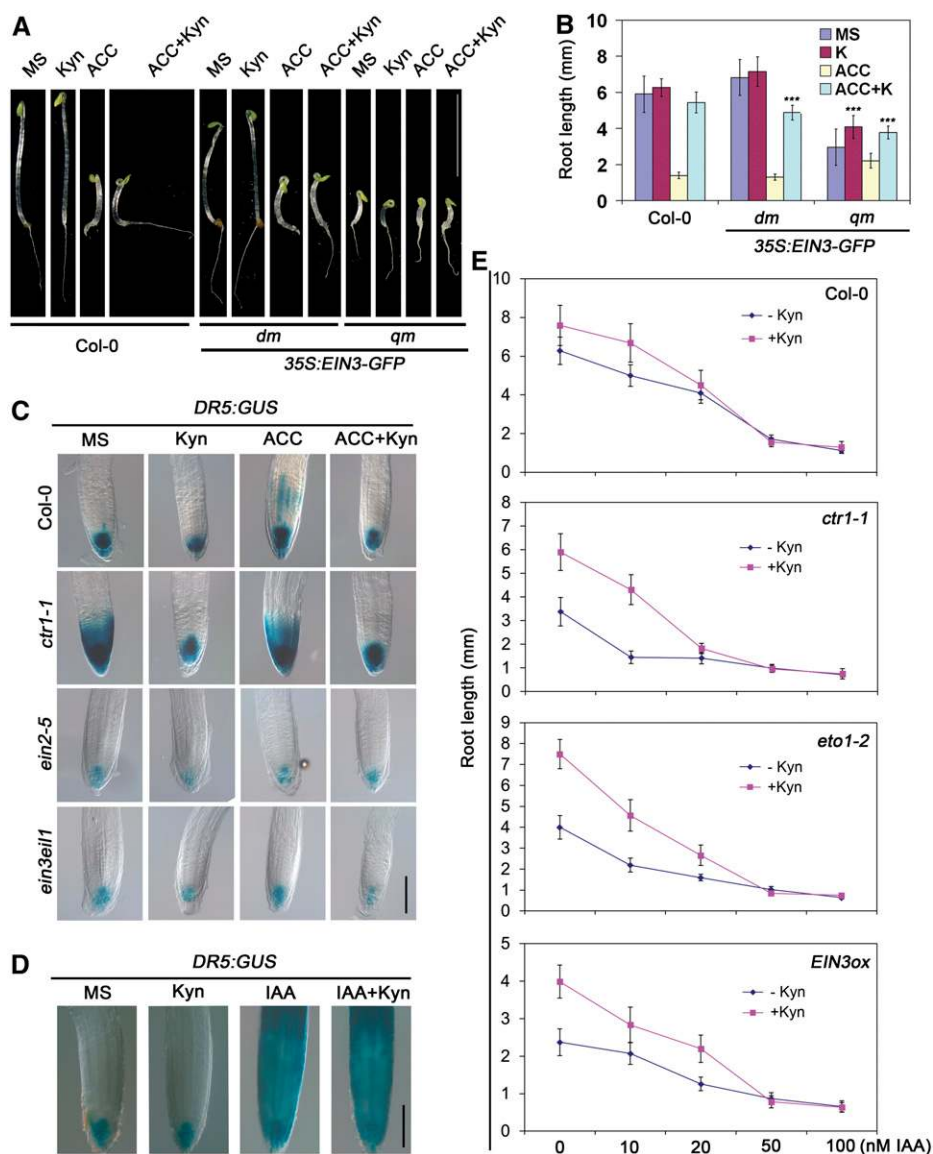


Figure 3. Kyn Decreases *DR5:GUS* Expression, but IAA Overrides Its Effect.

(A) Three-day-old etiolated seedlings of Col-0, *dm 35S:EIN3-GFP*, and *qm 35S:EIN3-GFP* grown on MS medium with or without Kyn (1.5 μ M) and/or ACC (10 μ M).

(B) Quantification of the root lengths of seedlings shown in **(A)** (Student's *t* test, between ACC and ACC+Kyn treatments for *dm EIN3-GFP* and *qm EIN3-GFP* and between Kyn-treated and nontreated *qm EIN3-GFP*; ****P* < 0.001).

(C) Expression of the *DR5:GUS* reporter in the roots of Col-0, *ctr1-1*, *ein2-5*, and *ein3eil1* backgrounds. The seedlings were grown in the dark for 3 d on MS medium with or without Kyn (1.5 μ M) and/or ACC (10 μ M). Bar = 100 μ m.

(D) Expression of the *DR5:GUS* reporter in the roots of 3-d-old etiolated Col-0 seedlings treated with Kyn (100 μ M) and/or IAA (10 μ M) for 3 h. Bar = 100 μ m.

(E) Root lengths of Col-0, *ctr1-1*, *eto1-2*, and *EIN3ox* etiolated seedlings grown on MS medium in the presence of a range of IAA concentrations with or without Kyn (1.5 μ M). Bars represent the average length (\pm SD) of at least 20 seedlings.

ethylene-insensitive mutant plants indicate that EIN3/EIL1-related ethylene signal is a major inducer of auxin accumulation or activity in root tissues, highlighting the importance of the ethylene pathway in maintaining the normal homeostasis and activity of auxin in roots.

We also assessed the effect of Kyn on other plant hormone pathways by examining *Thi2.1:GUS*, *ARR5:GUS*, and *RD29A:GUS*, widely used reporter lines for jasmonic acid, cytokinin, and ABA signals, respectively. As expected, the *GUS* expression in these lines was markedly induced by jasmonic acid, cytokinin,

and ABA, respectively. Lack of changes in GUS staining observed upon Kyn treatment in the presence of inducing hormone indicated the relatively specific function of Kyn in ethylene and auxin pathways (see Supplemental Figure 5 online).

Kyn Inhibits Ethylene-Induced IAA Biosynthesis

We next sought to determine which pathway of the auxin action (biosynthesis, transport, or signaling) is disturbed by Kyn. We first tested whether exogenous IAA can rescue the Kyn effect on *DR5:GUS* expression. As shown in Figure 3D, IAA treatment led to intensive GUS staining throughout the roots, and the repressive effect of Kyn was completely masked by the excess IAA treatment. This result suggests that Kyn treatment does not interfere with the perception of the IAA signal, but rather likely modulates IAA transport or biosynthesis. To test this possibility further, we quantified the root length of seedlings treated with a range of IAA concentrations in the presence or absence of Kyn (Figure 3E). When IAA concentrations were relatively low, root elongation stimulated by Kyn was still observed. Upon increasing IAA concentrations, the masking effect of IAA on the Kyn-stimulated root elongation became more evident. The effect of Kyn treatment in all backgrounds was completely blocked in the presence of 50 nM IAA. Together, these results strongly support that Kyn exerts its effect by affecting IAA biosynthesis or distribution.

We then measured the endogenous IAA levels in roots and found that ACC treatment markedly increased the level of endogenous IAA as previously reported (Růžička et al., 2007; Swarup et al., 2007), whereas Kyn application completely reversed the ACC effect and reduced the IAA accumulation even below the basal level (Figure 4A). These data provide direct evidence to support that Kyn inhibits ethylene-induced IAA accumulation in roots. We also examined the gene expression of some previously reported components involved in the ethylene-induced IAA biosynthesis pathway, such as *ASA1*, *TAA1*, and *TAR2*. In agreement with our preceding observation that Kyn inhibits EIN3 activity, we found that Kyn inhibited the expression of *ASA1:GUS*, *TAA1:GFP-TAA1*, and *TAR2:GUS*, particularly in the presence of ACC treatment (Figures 4B to 4D), further suggesting that Kyn inhibits ethylene-induced IAA biosynthesis. Nonetheless, Kyn only partly suppressed the ACC-induced expression of these IAA biosynthetic genes, which was in contrast with the considerably reduced IAA accumulation (Figure 4A). This discrepancy implies that Kyn might repress IAA accumulation by other means in addition to reducing the expression of those IAA biosynthetic genes.

To ascertain further the action of Kyn, we investigated whether the IAA biosynthetic enzymes could be targeted by Kyn. We first performed phenotypic analysis of a number of IAA biosynthetic mutants in the presence of exogenous Trp and/or Kyn. Trp is synthesized from chorismate via anthranilate (which is catalyzed

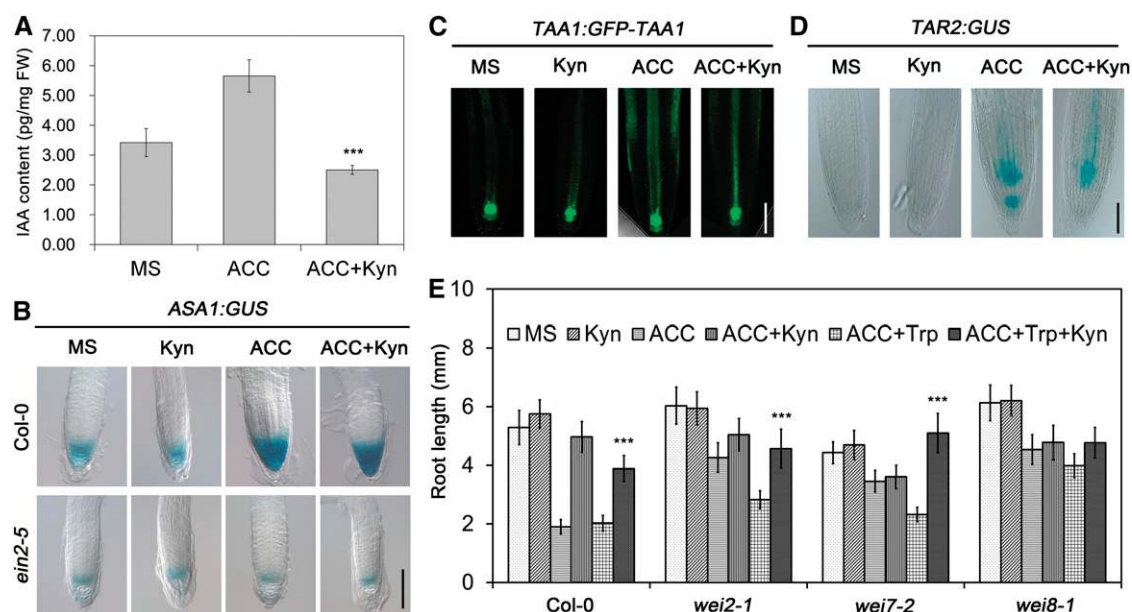


Figure 4. Kyn Inhibits Ethylene-Induced IAA Biosynthesis.

(A) IAA levels in the roots of 3-d-old etiolated seedlings grown on ACC (10 μ M) and/or Kyn (1.5 μ M) plates. Bars represent mean \pm SD ($n = 3$, Student's t test, between ACC and ACC+Kyn treatments; *** $P < 0.001$). FW, fresh weight.

(B) GUS staining in the roots of *ASA1:GUS* and *ein2-5 ASA1:GUS*. Bar = 100 μ m.

(C) GFP fluorescence in the roots of *TAA1:GFP-TAA1*. Bar = 50 μ m.

(D) GUS staining in the roots of *TAR2:GUS*. Bar = 50 μ m. The 3-d-old etiolated seedlings in (B) to (D) were grown on MS medium or MS supplemented with Kyn (1.5 μ M) and/or ACC (10 μ M).

(E) Root lengths of Col-0, *wei2-1*, *wei7-2*, and *wei8-1*. The 3-d-old etiolated seedlings were grown on MS medium with different combinations of Kyn (1.5 μ M), ACC (0.5 μ M), and Trp (10 μ M). Bars represent the average length (\pm SD) of at least 20 seedlings (Student's t test, between ACC+Trp and ACC+Trp+Kyn treatments; *** $P < 0.001$).

by ASA1/WEI2 and ASB1/WEI7) and serves as the substrate of the WEI8/TAA1-catalyzed reaction in IAA biosynthesis. As previously reported, Trp addition (10 μ M) restored the ethylene sensitivity of *wei2-1* and *wei7-2*, but not *wei8-1* (Figure 4E). We further found that Kyn reversed this Trp effect on the *wei2* and *wei7* mutants (Figure 4E), suggesting that the possible target site of Kyn lies downstream of Trp synthesis involving ASA1 and ASB1.

Kyn Is a Potent Inhibitor of TAA1/TAR Aminotransferases

Importantly, Kyn had no obvious effect on the root elongation of *wei8* compared with *wei2* or *wei7* in the presence of low doses of ACC (Figure 4E), suggesting that TAA1 could be a potential target of Kyn. To explore this possibility further, we determined whether Kyn affects the enzymatic activity of an *Escherichia coli*-purified TAA1. The kinetics analysis showed that the K_i of TAA1 by Kyn (11.52 μ M) is remarkably lower than the K_m of TAA1 to Trp (61.61 μ M), indicating the potent inhibitory effect of Kyn on TAA1 in vitro (Figure 5A). The Dixon plot also showed that the inhibition is competitive (Figure 5A). Notably, we found that TAA1 could also use Kyn as a substrate in vitro to produce kynurenic acid (KYNA), a direct metabolite of Kyn in animals (Beadle et al., 1947) (Figure 5C). This result suggests that, like Trp, Kyn is a TAA1 substrate. However, unlike Kyn, KYNA is not a TAA1 substrate and showed no effect on TAA1 activity (see Supplemental Figure 6A and B online), nor did it influence the root growth phenotypes (see Supplemental Figure 6C online). Likewise, several other known Kyn derivatives in animals, such as quinolinic acid, NAD⁺, nicotinamide, and nicotinic acid (Kato and Hashimoto, 2004) (see Supplemental Figure 6D online), did not promote the root elongation of the *ctr1-1* seedlings (see Supplemental Figure 6E online). Based on these results, we conclude that Kyn, but not its metabolites, is an alternate substrate of TAA1 that potently and competitively inhibits TAA1 activity.

Multiple *wei8* mutant alleles were found to be hypersensitive to Kyn treatments, whereas Col *TAA1:GFP-TAA1* plants that harbor extra copies of TAA1 were hyposensitive to Kyn treatments in terms of root elongation (Figure 5D), suggesting that TAA1 is not the only target of Kyn. We then examined the effect of Kyn on the enzymatic activity of TAA1-related proteins (TARs), which are expected to have similar functions as TAA1 (Stepanova et al., 2008). Although we failed to purify TAR2 from *E. coli*, we found that the *E. coli*-expressed TAR1, like TAA1, possessed aminotransferase activity in vitro, and Kyn efficiently inhibited its activity (Figure 5E). TAR1 was also able to convert Kyn into KYNA (Figure 5E), suggesting that at least in vitro, Kyn can be used as an alternate substrate by TAA1 and TAR1. This, together with the kinetic properties shown in Figure 5A, indicates that Kyn functions as an alternate substrate that can competitively inhibit TAA1/TAR-mediated conversion of Trp into IPyA.

To demonstrate the inhibitory effect of Kyn on TAA1/TARs further, we compared the phenotypes of Kyn-treated wild-type seedlings with those of *wei8* and *wei8 tar2*. It was reported that the *wei8 tar2* mutant seedlings display various growth defects due to the reduced synthesis of endogenous IAA, including small and upward-curved cotyledons and shortened hypocotyls and roots (Stepanova et al., 2008) (Figures 6A and 6B). We found that the wild-type seedlings upon 10 μ M Kyn treatment and the

wei8-1 seedlings upon 1 μ M Kyn treatment exhibited a growth retardation phenotype almost identical to *wei8 tar2* (Figure 6A). Similarly, the cotyledons of 8-d-old wild-type seedlings treated with 100 μ M Kyn showed a distinct upward curvature phenotype that was observed in *wei8 tar2* (Figure 6B). These results indicate that Kyn treatment largely mimics the loss of TAA1/TAR functions, suggesting Kyn as a potent inhibitor effectively targeting TAA1-related Trp aminotransferases in plants.

Computational Docking and Molecular Modeling Reveal That Kyn Competitively and Selectively Inhibits TAA1/TAR Activity

To explore the mechanism of Kyn inhibition on TAA1-like aminotransferases further, we investigated the interaction between Kyn and TAA1 by molecular docking and modeling. We separately modeled the interaction between Kyn and KAT1 (a structurally resolved aminotransferase in human that could recognize and catalyze Kyn; PDB ID:1W7L) (Han et al., 2009) (Figure 7A), Kyn and TAA1 (PDB ID:3BWN; Figure 7B), and Trp and TAA1 (Figure 7C). The hydrogen bond networks between TAA1 and Kyn/Trp are similar: The phosphate oxygen atom of LLP217 forms a hydrogen bond with nitrogen linked directly to the benzene ring of the small ligand; oxygen of Tyr-129 forms a hydrogen bond with the α -NH₂ of the ligand; and the amino groups of Arg-350 and Arg-363 form hydrogen bonds with oxygen of α -COOH (Figures 7B and 7C). The only difference between the two ligands is that Kyn could also form intramolecular hydrogen bonds. In addition, Kyn/Trp may form hydrogen bonds with Gly-30, Asn-168, and Thr-131, as the small ligands may dynamically change their positions before binding to catalytic sites (e.g., from suboptimal position to optimal binding position). The docking results suggest that Kyn could bind to the catalytic pocket of TAA1 similarly to Trp. The free energy of binding for these three interactions is similar: KAT1 and Kyn (−7.73 kcal/mol), TAA1 and Kyn (−7.72 kcal/mol), and TAA1 and Trp (−7.55 kcal/mol) (see Supplemental Table 1 online). The docking model and lower binding energy of Kyn and TAA1 interaction (meaning Kyn and TAA1 form more favorable binding and, thus, tighter electrostatic and hydrogen bonding networks) suggest that Kyn is a potent competitive inhibitor of TAA1. Consistent with the competitive inhibition model, when *ctr1*, *eto1*, and EIN3ox seedlings were grown in the presence of high doses of Trp (100 μ M or 1 mM), Kyn was no longer able to reverse the root growth defects of these lines (see Supplemental Figure 7 online). These data suggest that Trp outcompetes Kyn and is consistent with Kyn working as a competitive inhibitor of TAA1/TAR activity.

By structure alignment of TAA1 and KAT1 based on their three-dimensional structural similarity (Figure 7D), LLP217, Tyr-194, Asn-168, Arg-363, and Gly-30 in TAA1 were found at virtually the same positions as the same residues in KAT1 that directly interact with Kyn. Among these core amino acids, LLP217, Asn-168, and Arg-363 have also been predicted to participate in substrate binding (Tao et al., 2008). That Tyr-194, instead of Tyr-129, is identified as a conserved amino acid in the structure alignment indicates the possible conformational change of TAA1 when binding to its ligand. Among these residues, the hydroxyl

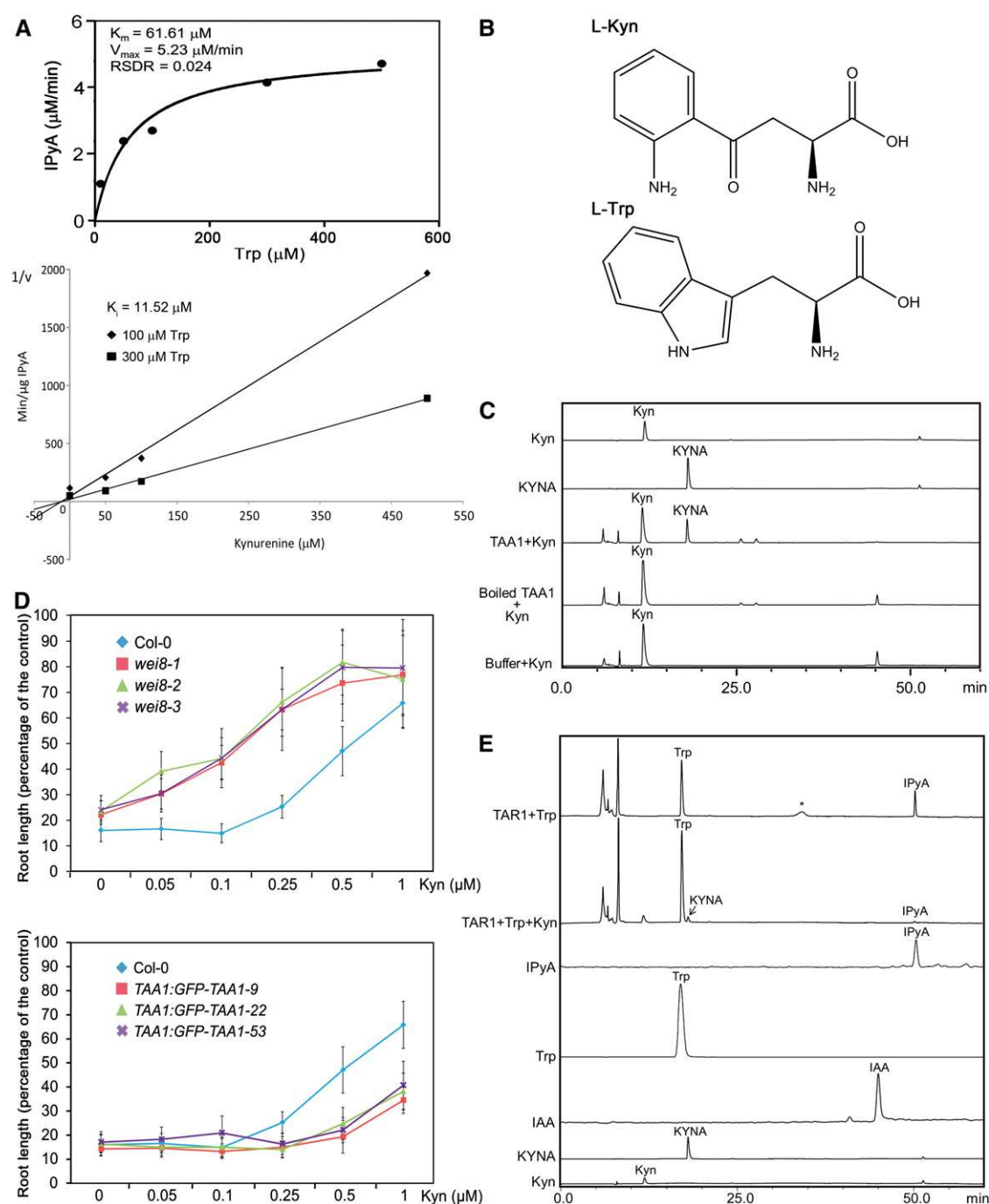


Figure 5. Kyn Potently and Competitively Inhibits TAA1/TAR1 Activity.

(A) Kyn competitively inhibits TAA1 activity in vitro. The K_m and V_{max} for TAA1 using Trp as a substrate (top). K_i for the Kyn-mediated inhibition of TAA1 activity was determined using a Dixon plot (bottom).

(B) The chemical structure of Kyn (top) and Trp (bottom).

(C) Kyn is a substrate of TAA1. HPLC analysis of the Kyn and KYNA standards and of the reaction products when Kyn (500 μM) is used as a substrate with purified recombinant GST-TAA1 or boiled GST-TAA1. Absorbance at 280 nm is shown.

(D) TAA1 loss-of-function mutants are hypersensitive to Kyn, while transgenic plants with multiple copies of TAA1 are hyposensitive to Kyn. Dose-response curves for the relative root lengths of three *wei8* mutant alleles (top) and three independent transgenic *TAA1:GFP-TAA1* lines (bottom). All seedlings were grown for 3 d in dark on MS medium supplemented with ACC (10 μM) and Kyn (from 0 to 1 μM), and the root lengths of respective genotypes grown on MS were used as controls. Bars represent the average length ($\pm\text{SD}$) of at least 30 seedlings.

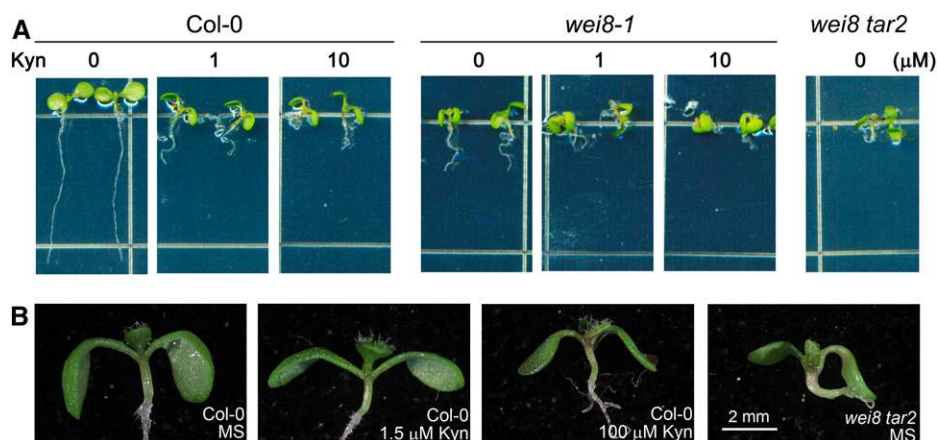


Figure 6. Phenotypic Analysis Indicates the Similarity between Kyn-Treated Wild-Type and Untreated *wei8 tar2* Seedlings.

(A) Six-day-old seedling phenotype of Col-0, *wei8-1*, and *wei8 tar2* grown on vertical plates supplemented with increasing Kyn concentrations. More than 10 seedlings of every plate were observed, and two representative seedlings are shown.

(B) Cotyledon phenotype of 8-d-old Col-0 and *wei8 tar2* seedlings grown on MS medium supplemented without or with increasing Kyn concentrations. Note that Col-0 seedlings treated with 100 μ M Kyn showed a distinct cotyledon upward curve phenotype also observed in *wei8 tar2*. More than 10 seedlings of every plate were observed. Bar = 2 mm.

group of PLP, which is linked with Lys-217, is also essential for stabilizing the α -NH₂ of Kyn or Trp near the reaction center (Cerqueira et al., 2011). The phosphate oxygen atom of LLP217 forms a hydrogen bond with nitrogen linked directly to the benzene ring of the Kyn, suggesting that LLP217 mainly determines the TAA1 selectivity toward Kyn, while the other four core residues interact with α -NH₂ or α -COOH of Kyn, thus providing no selection of amino acids. As expected, these five key residues responsible for Kyn binding were conserved in all members of the *Arabidopsis* TAA1 family (Figure 7E), implying that all TAA1-like aminotransferases are inhibited by Kyn. We also aligned the TAA1 sequence with other plant aminotransferases in *Arabidopsis* annotated by SwissProt (<http://www.uniprot.org>) (see Supplemental Figure 8 online). Notably, the core LLP217 residue is not conserved in any other families of these aminotransferases (Figure 7F; see Supplemental Figure 8 online). In the Tyr aminotransferase family, except for LLP217 residues, the other four predicted hydrogen bond-forming residues are conserved (Figure 7F), whereas in other families of *Arabidopsis* aminotransferases, there is little conservation of Kyn binding residues (see Supplemental Figure 8 online). Collectively, our sequence alignment results suggested that other aminotransferase family proteins, including ACS enzymes, might not be targets of Kyn. Further support came from an in-gel Trp aminotransferase activity assay showing that while Kyn efficiently repressed activity of the recombinant TAA1 protein, it did not influence an endogenous *E. coli* aminotransferase (see Supplemental Figure

9 online), suggesting some degree of specificity of Kyn with respect to TAA1.

IAA Stabilizes EIN3 Protein in an EBF1/2-Dependent Manner

The aforementioned data demonstrate that Kyn has dual effects in antagonizing ethylene-induced root inhibition: It decreases EIN3 accumulation and inhibits TAA1-mediated auxin biosynthesis. To clarify whether these two types of regulation are interconnected, we investigated whether Kyn destabilizes EIN3 through its effect on auxin biosynthesis. We found that application of IAA can strongly suppress the effect of Kyn on EIN3 nuclear accumulation in the root tips and elongation zones of *ein3 eil1 35S:EIN3-GFP* (Figure 8A), indicating that increased auxin levels enhance EIN3 accumulation. Consistent with the notion that Kyn attenuates EIN3 accumulation by altering auxin levels, we found that whereas Kyn effectively suppressed ACC-induced EIN3 accumulation, further addition of IAA fully reversed the effect of Kyn. In fact, the concurrent presence of ethylene and IAA led to a greater EIN3 stability (Figure 8B). We also showed that IAA, but not ACC, enhanced EIN3-GFP accumulation in the *ein2 ein3 eil1* background (Figure 8C; see Supplemental Figure 10C online), which is completely insensitive to ethylene (An et al., 2010). Conversely, the same IAA treatment of *ein3 eil1 ebf1 ebf2 35S:EIN3-GFP* caused no obvious augmentation of EIN3 accumulation (Figure 8D), suggesting that auxin-induced EIN3 accumulation is EBF1/2 dependent. Our previous study revealed that

Figure 5. (continued).

(E) Kyn also inhibits TAR1 activity and is a TAR1 substrate. HPLC analysis of Trp, IPyA, IAA, Kyn, and KYNA standards and of the reaction products catalyzed by purified recombinant GST-TAR1. Absorbance at 280 nm is shown.

All the enzymatic activities were assayed by the HPLC analysis and quantification of the IPyA reaction products. Each data point represents at least two independent samples. These experiments were repeated at least twice with similar results.

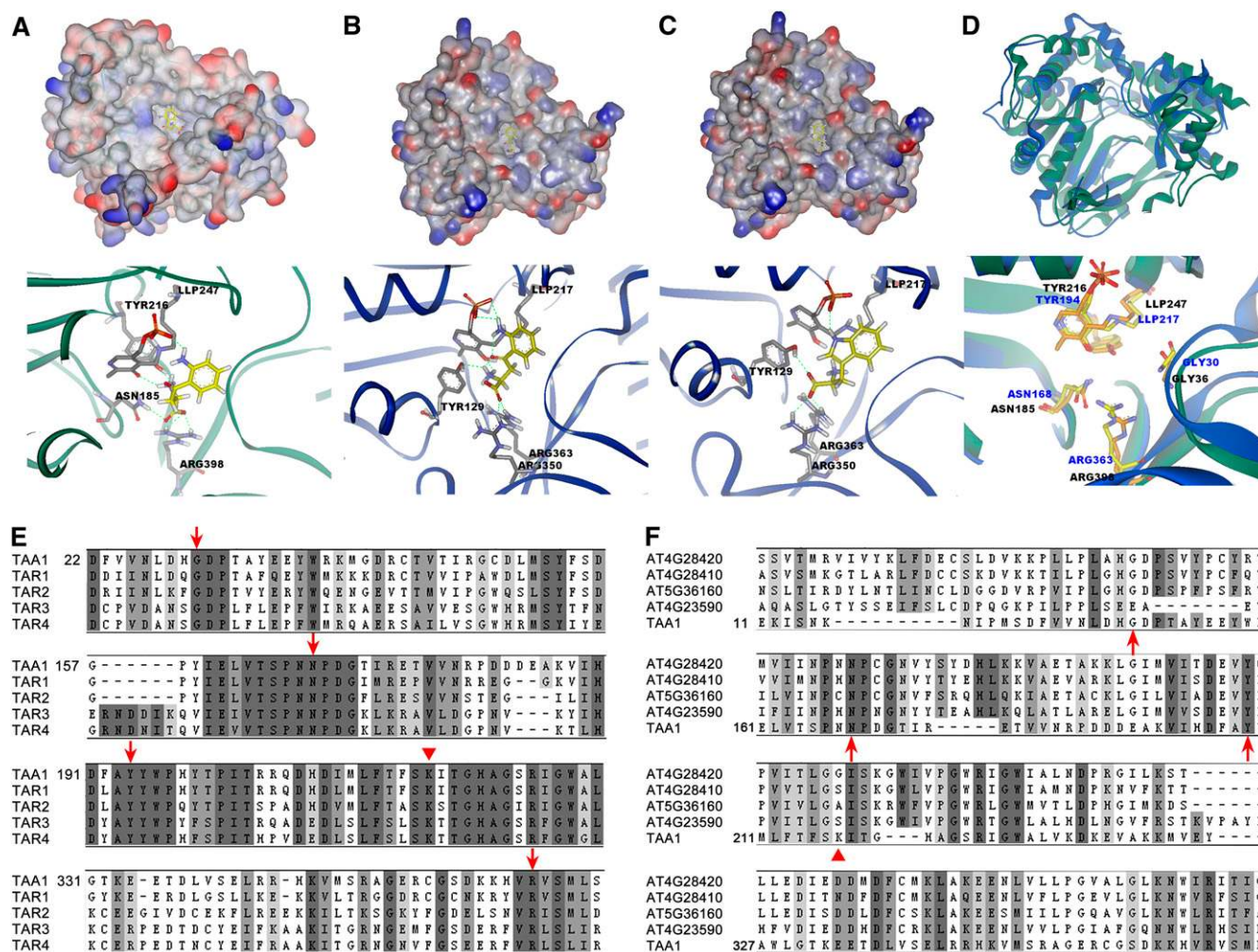


Figure 7. Molecular Docking Reveals That Kyn Competitively and Selectively Inhibits TAA1/TAR Activity.

(A) Molecular structure illustrating the interaction between Kyn and KAT1.

(B) Molecular modeling of the interaction between Kyn and TAA1, illustrating that Kyn could fit within the catalytic pocket of TAA1.

(C) Molecular modeling of the interaction between Trp and TAA1.

The top panels of **(A)** to **(C)** show the interaction between the small ligands (in yellow) and the catalytic pockets of the receptors (in gray). Bottom panels show the key residues that contribute to the binding with these proteins.

(D) The structure alignment of TAA1 and KAT1 shows that they are very similar at binding sites for small ligands. TAA1 is shown as a blue ribbon with yellow side chains, while KAT1 is shown as a green ribbon with orange side chains. Bottom panel shows the details of key amino acids of TAA1 and KAT1 responsible for recognizing and binding to Kyn and/or Trp.

(E) and **(F)** The multiple sequence alignment data show that the core amino acids in **(D)** (Lys-217, marked by red triangle; Gly-30, Tyr-194, Asn-168, and Arg-363, tagged with red arrowhead) are all conserved in the *Arabidopsis* TAA1/TAR family **(E)**, whereas Lys-217 is not conserved in Tyr aminotransferases **(F)**. The dark-colored boxes correspond to identical and partially conserved amino acids.

ethylene enhances EIN3 accumulation via the destabilization of EBF1 and EBF2 (An et al., 2010). However, IAA seemed to use a distinctive mechanism from ethylene to stabilize EIN3, as it did not destabilize EBF1-GFP or EBF2-GFP while promoting EIN3 accumulation in the *ein2* background (see Supplemental Figures 10A and 10B online). Collectively, these findings arguably favor the possibility that Kyn destabilizes, whereas auxin stabilizes, EIN3 protein at least partly through the regulation of ethylene signaling, which is also supported by the ability of Kyn to

suppress *ctr1* in terms of root phenotype and *EBS:GUS* expression (Figures 1 and 2B).

DISCUSSION

Although the linear model of a canonical early ethylene signal transduction pathway has now been firmly established, the investigation of downstream signaling events and regulatory networks is just beginning. Taking advantage of the power of

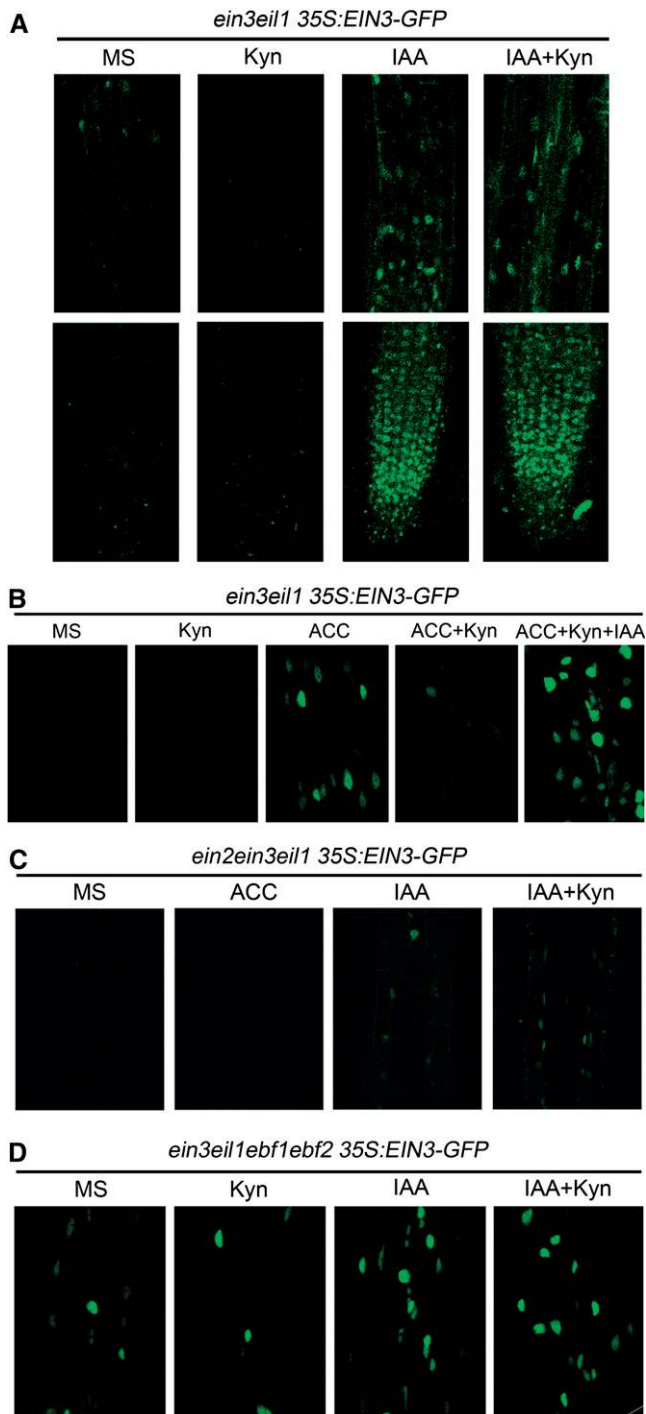


Figure 8. IAA Stabilizes EIN3 Accumulation in the Nuclei of Root Tissues.

(A) GFP fluorescence in the elongation zones (top) and root tips (bottom) of *ein3 eil1 35S:EIN3-GFP*, showing that IAA stabilizes EIN3 accumulation.

(B) Kyn suppresses ACC-induced EIN3-GFP accumulation, whereas IAA reverses Kyn-mediated suppression in *ein3 eil1 35S:EIN3-GFP*.

(C) IAA can, but ACC cannot, augment EIN3-GFP accumulation in the *ein2 eil3 eil1* background.

chemical genetics, we performed a small-molecule library screen and identified Kyn for its ability to suppress the ethylene responses and inhibit EIN3 accumulation in *Arabidopsis* root tissues. Further in vitro enzymatic analysis and in vivo functional studies revealed that Kyn competitively inhibits TAA1/TAR aminotransferase activity in the IPyA pathway of auxin biosynthesis. Additional phenotypic analysis showed that Kyn treatment largely mimics the loss of TAA1/TAR functions, and molecular modeling and computational docking experiments validated the potency and selectiveness of Kyn in targeting TAA1/TARs but not other families of aminotransferases. We also uncovered a new mode of interaction between auxin and ethylene, wherein auxin exerts positive feedback regulation on its own synthesis through enhancing EIN3 protein accumulation.

Kyn is an intermediate product of the Trp degradation pathway in animals. Kyn, KYNA (one branch of Kyn metabolism), 3-hydroxykynurenine, and quinolinic acid (another branch of Kyn metabolism) are all neuroactive compounds that play important roles in neurodegenerative disorders, including Alzheimer's and Huntington's diseases (Schwarcz et al., 1983; Foster et al., 1984; Sas et al., 2007). Recently, the augmentation of the KYNA-to-3-hydroxykynurenine ratio by genetic or pharmacological approaches was shown to have potential therapeutic benefits in both fly and mouse Huntington's disease models (Campesan et al., 2011; Zwillig et al., 2011). However, it has been reported that most core enzymes in Kyn metabolism could not be found in the *Arabidopsis* genome (Kato and Hashimoto, 2004).

Our study revealed that Kyn represses ethylene responses, particularly effectively in roots. Much higher concentrations of Kyn are required to suppress ethylene-induced hook bending, suggesting the existence of sensitivity differences in root/shoot tissues or a restriction of efficient Kyn transport from root to shoot. The robust inhibition of ethylene responses in *eto1*, *ctr1*, and ACC-supplied wild-type seedlings suggested that Kyn modulates the activity of the ethylene signaling pathway downstream of CTR1, rather than affecting the upstream ethylene biosynthesis pathway. Further studies revealed that Kyn downregulates the levels of EIN3 protein and also inhibits the auxin biosynthesis pathway. Several lines of evidence support the latter conclusion. First, the ethylene-induced *DR5:GUS* expression and IAA levels are abrogated by Kyn application. Second, IAA treatment rescues the effect of Kyn on *DR5:GUS* expression as well as on root growth inhibition, suggesting that Kyn leads to a reduction in auxin accumulation rather than transport or signaling. Third, Kyn suppresses the ethylene-induced IAA accumulation level in roots and inhibits the expression of *WEI2*, *WEI8*, and *TAR2*. Finally and most importantly, we found that Kyn potently and competitively inhibits TAA1/TAR activity, likely by competing with the endogenous substrate Trp. Kyn treatment mimics the loss of TAA1/TAR functions in terms of morphological phenotypes and enzymatic activity analysis. A molecular modeling approach revealed that Kyn nicely fits into the substrate

(D) IAA and/or Kyn have no effect on EIN3-GFP accumulation in the *ein3 eil1 ebf1 ebf2* background. Three-day-old etiolated seedlings of indicated genotypes were treated with Kyn (100 μ M), ACC (100 μ M), and/or IAA (10 μ M) for 3 h before fluorescence microscopy.

pocket of TAA1, and the five core residues for Kyn interaction are conserved in all members of the TAA family but not in other families of *Arabidopsis* aminotransferases. Therefore, our data report Kyn as a newly identified auxin biosynthetic inhibitor that effectively and selectively targets TAA1-like Trp aminotransferases.

Although a number of small molecules have been identified to modulate hormone responses effectively (reviewed in Tóth and van der Hoorn, 2010), the identification of the direct targets of these chemicals still remains a great challenge in most cases. Kyn is one of the few small molecule inhibitors with identified targets and mode of action. Our *in vitro* kinetic analysis indicated that Kyn potently inhibits TAA1/TAR activity. Our *in vivo* data also support this finding, as the seedling phenotypes of the wild type treated with high concentrations of Kyn are quite similar to *wei8 tar2* loss-of-function mutant, further indicating that Kyn mainly targets TAA1/TARs.

The morphological phenotypes caused by Kyn treatment, particularly at the 1 μ M level, illustrate that Kyn is a highly effective but relatively nontoxic compound for seedlings, which makes Kyn clearly different from other hormone inhibitors that exhibit strong side effects. For instance, AVG, a widely used inhibitor of ACSs, has recently been reported to be an inhibitor of Trp aminotransferase activity (Soeno et al., 2010), but it is likely to affect all or most PLP-dependent enzymes, therefore limiting its use in pharmacological experiments. By contrast, Kyn seems to affect largely if not solely TAA1-like Trp aminotransferases based on the phenotypic analysis. The molecular docking data further support that Kyn selectively inhibits TAA1/TAR activity as it fits into the TAA1/TAR substrate binding pocket. Due to the lack of five conserved residues involved in Kyn recognition, it is believed that Kyn can target only the TAA1/TAR family of plant aminotransferases but not other related families. In line with this target specificity, Kyn failed to inhibit the function of an *E. coli* aminotransferase *in vitro*. Meanwhile, Kyn directly inhibits plant TAA1/TAR activity, as none of the Kyn-related metabolites affect ethylene-induced root inhibition nor does its immediate metabolite KYNA inhibit the enzymatic activity of TAA1. The identification of Kyn as a relatively specific and highly effective inhibitor of TAA1/TARs in our study would thus provide a new route to explore and exploit TAA1/TAR-mediated auxin biosynthesis.

Previous studies in animals demonstrate that Trp, IPyA, and IAA, all being structural analogs of Kyn, competitively inhibit kynurenine aminotransferase1 (KAT1), which catalyzes the conversion of Kyn into KYNA (Han et al., 2009). Given the structural similarity between Kyn and the TAA1 substrate, Trp, as well as between KAT1 and TAA1, we propose a competitive inhibition mechanism of TAA1 by Kyn, which is consistent with the finding that high concentrations of Trp (100 μ M and 1 mM) can suppress Kyn's root-promoting effect. This idea is further supported by the *in vitro* results showing that Kyn is a TAA1/TAR1 substrate that competitively inhibits the conversion of Trp into IPyA. Therefore, due to their structural similarity, Kyn and Trp likely behave as antagonists to each other in both animals and plants.

The complex interactions between auxin and ethylene have been long studied. On one hand, excessive auxin application was found to increase ethylene biosynthesis by inducing the expressions of multiple ACS genes (Abel et al., 1995; Tsuchisaka and Theologis, 2004). On the other hand, ethylene was reported to

induce auxin local biosynthesis, transport, or signaling (Stepanova et al., 2005, 2007, 2008; Růžička et al., 2007; Swarup et al., 2007). Using Kyn as a potent inhibitor of TAA1/TARs, we uncover a new mode of auxin-ethylene interplay: Auxin can positively regulate the ethylene signaling pathway to accelerate its own biosynthesis. The observations that IAA, but not ACC, stabilizes EIN3-GFP in the *ein2 ein3 eil1* background and that Kyn inhibits the phenotypes of *ctr1* all point to a scenario in which auxin is able to enhance ethylene signaling in addition to its production. Auxin seems to promote EIN3 accumulation by suppressing EBF1/2-mediated EIN3 protein degradation. However, unlike ethylene, auxin does not affect EBF1/2 accumulation, suggesting that the two types of hormones employ distinct mechanisms to stabilize EIN3. Currently, the molecular details of auxin regulation of EIN3 stability are not clear and await further investigation.

We also noted that *DR5:GUS* expression is marginal in the *ein2* and *ein3 eil1* mutant backgrounds, and Kyn has no effect on either *DR5:GUS* expression or root lengths of these mutants,

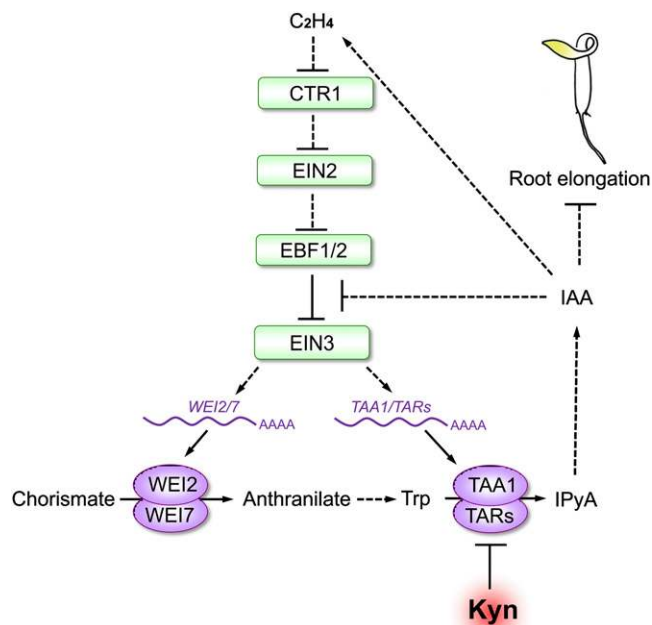


Figure 9. A Proposed Model Illustrating the Interaction between Ethylene Signaling and Auxin Biosynthesis in the Regulation of Root Elongation.

Ethylene acts to stabilize EIN3 through its canonical signaling pathway, and the accumulated EIN3 transcription factor activates the expression of several auxin biosynthetic genes, including *WEI2*, *WEI7*, *TAA1*, and *TAR2*. *WEI2* and *WEI7* are required for Trp production, while *TAA1* and *TAR2* (and probably other TARs as well) convert Trp into IPyA, which eventually leads to the synthesis of IAA and the inhibition of root elongation. In addition to promoting ethylene biosynthesis, IAA is also able to enhance EIN3 stability probably by repressing EBF1/2-mediated EIN3 degradation, forming a positive feedback loop between ethylene signaling and auxin biosynthesis. Kyn has been identified in this study as a small compound that competitively and selectively inhibits the family of TAA1/TARs.

[See online article for color version of this figure.]

suggesting that the EIN3/EIL1-relayed ethylene signal is a principal inducer of local auxin synthesis in roots. Based on our study, a working model is proposed (Figure 9) in which auxin acts to stabilize EIN3 (by enhancing both ethylene production and signaling pathways) and forms a positive feedback loop to increase its own synthesis, particularly in root tissues. This model also provides a possible explanation for how Kyn antagonizes ethylene's effect on EIN3 protein accumulation and root elongation (i.e., by decreasing TAA1-mediated auxin production). Auxin gradients are established via polar transport and local biosynthesis and thought to be a key regulatory mechanism of plant growth and development (Benjamins and Scheres, 2008; Zhao, 2010). Maintenance of local auxin accumulation or maxima relies on multiple positive feedback regulations. For instance, in the organogenesis process, auxin maxima are maintained by inducing the gene expression of *PIN1* at the shoot apical meristem, which in turn facilitates polar auxin transport to enhance local auxin accumulation further (Reinhardt et al., 2003; Jönsson et al., 2006; Smith et al., 2006). In leaf epidermal pavement cells, ROP2 and PIN1 participate in a positive feedback loop to maintain the asymmetric accumulation of auxin and cause lobe formation at the fringe of PIN localization (Xu et al., 2010). Our work demonstrates a previously undiscovered positive feedback loop between the auxin biosynthesis and ethylene signaling pathways in roots, providing an additional layer of regulatory mechanisms in the complexity of auxin action.

METHODS

Plant Materials and Growth Conditions

All *Arabidopsis thaliana* mutants and transgenic lines employed in this study are in the Col-0 background. *ctr1-1* (Kieber et al., 1993), *eto1-2* (Guzmán and Ecker, 1990), *EIN3ox* (Chao et al., 1997), *ein2-5* (Alonso et al., 1999), *ein3-1 eil1-1* (Alonso et al., 2003), *ebf2-1* (Guo and Ecker, 2003), *ein3-1 eil1-3 ebf1-1 ebf2-1* (An et al., 2010), *wei2-1* (Stepanova et al., 2005), *wei7-2* (Stepanova et al., 2005), *wei8-1*, *wei8-2*, and *wei8-3* (Stepanova et al., 2008), *wei8-1^{+/-} tar2-1^{-/-}* (Stepanova et al., 2008), *EBS:GUS* (Stepanova et al., 2007), *DR5:GUS* (Quaedvlieg et al., 1998), *Thi2.1:GUS* (Epple et al., 1995), *ARR5:GUS* (D'Agostino et al., 2000), *ASA1:GUS*, *ein2-5 ASA1:GUS*, *ASB1:GUS*, *ein2-5 ASB1:GUS*, *TAA1:GFP-TAA1*, *TAR2:GUS* (Stepanova et al., 2005, 2008), and *ein2 GFP-EBF2* (An et al., 2010) lines were described previously. *ein2 EBF1-GFP*, *ein3 eil1 EIN3-GFP*, and *ein3 eil1 ebf1 ebf2 EIN3-GFP* were constructed by *Agrobacterium tumefaciens*-mediated transformation of the pCHF3-EBF1-GFP construct (An et al., 2010) or pCHF3-EIN3-GFP construct (Guo and Ecker, 2003) into *ein2* or *ein3 eil1* and *ein3 eil1 ebf1 ebf2* plants. Homozygotes were identified based on kanamycin resistance, GFP fluorescence, and genotyping. *RD29A:GUS* used in Supplemental Figure 5C online was constructed by inserting the promoter of *RD29A* (primers: 5'-ACGCGTCGACCCCGACCGACTACTAATAATAG-3' and 5'-CGGGA-TCCCCGACCGACTACTAATAATAG-3') into pB1101.1 and then transformed into Col. Double mutants or multiple genotype combinations (*ctr1-1 EBS:GUS*, *ein2-5 EBS:GUS*, *ein3-1 eil1-1 EBS:GUS*, *EIN3ox EBS:GUS*, *ctr1-1 DR5:GUS*, *ein2-5 DR5:GUS*, and *ein3-1 eil1-1 DR5:GUS*) were generated by genetic crosses. The homozygous lines were identified by phenotype and genotype screening with the methods provided in the respective references.

Surface-sterilized seeds were sown on Murashige and Skoog (MS) medium (4.3 g/L MS salts, 10 g/L Suc, pH 5.7 to 5.8, and 8 g/L agar

supplemented with the indicated concentrations of Kyn, ACC, IAA, and/or Trp and imbibed at 4°C for 3 d. For the assays conducted with etiolated seedlings, plates were kept under light for 3 to ~4 h after imbibition to promote seed germination, wrapped with aluminum foil, and incubated in the dark at 22°C for 3 d. In transient treatment experiments, the 3-d-old etiolated seedlings were transferred into liquid MS medium supplemented with the indicated chemicals and then incubated in the dark for 3 to 4 h. For light-grown seedlings, the plates were placed at 22°C with a 16 h-light/8 h-dark illumination cycle after a 5-d-long imbibition.

Small Molecule Library and Screen Information

The small molecule library screen was performed at the University of California at Riverside using the selected 2000 diverse chemicals in a microsource spectrum (SP 2000, <http://www.msdiscovery.com>) with an average stock concentration of 0.5 mg/100 μ L chemicals in DMSO. The spectrum collection can be downloaded from the following website (<http://www.msdiscovery.com/downloads.html>). Each chemical in this pool has been well characterized with specific structures, formula, molecular weight, market names, and functions. The library was screened at a concentration of 50 to 100 μ M in 200 μ L of liquid MS medium using standard 96-well microplates. *Arabidopsis* seeds (*eto1-2*, *ctr1-1*, and Landsberg *erecta* and Col-0 controls) were sterilized by 75% ethanol with 0.05% Triton X-100 for 10 min, then sedimented and resuspended in 95% ethanol for <2 min. Seeds were transfer onto filter papers in a hood to dry. Five to ten sterilized seeds/well were put into 96-well plates with liquid MS and stored at 4°C for 3 d. Chemicals were then added by automated robot (Beckman Coulter Biomek FX) from 384-well plates to 96-well plates, with DMSO as a control. Seedlings were grown in the dark for 3 d in the presence of chemicals. An initial screen was started by looking for seedlings with longer roots and/or hypocotyls in each well. A secondary screen was performed to confirm the effect of interesting candidate chemicals. We used ChemMine (<http://bioweb.ucr.edu/ChemMineV2/>) (Girke et al., 2005) to locate corresponding chemicals for each well.

Chemical Solutions

All chemicals used in this work were from Sigma-Aldrich. The stock solutions were prepared at the concentration indicated and filtered with 22-nm sterilized filters: Kyn (50 mM), ACC (10 mM), IAA (1 mM), Trp (100 mM), KYNA (50 mM), methyl jasmonate (100 mM), KT (1 mg/mL), and ABA (5 mM). Kyn and KYNA were dissolved in DMSO, and the TAA1 enzymatic inhibition experiments (in Figure 5 and Supplemental Figure 9 online) were done using 50 mM Kyn in 0.1 N HCl. Methyl jasmonate was dissolved in ethanol, whereas other chemicals were dissolved in water. The final concentrations of the chemicals are indicated in the respective figure legends. For Kyn, a range of concentrations (from 0.01 to 1000 μ M) in MS medium was tested to determine an optimal dose for triggering distinct phenotypes, and 1.5 μ M was used in most cases unless otherwise indicated.

GUS Staining

Seedlings were grown on the indicated medium for 3 d in the dark or 5 d under light, then were collected and washed with staining buffer without X-Gluc and stained with GUS staining buffer (50 mM sodium phosphate buffer, pH 7.0, 10 mM Na₂EDTA, 0.5 mM K₄[Fe(CN)₆] \cdot 3H₂O, 0.5 mM K₃[Fe(CN)₆], 0.1% Triton X-100, and 1 mg/mL X-Gluc). Ethanol (70%) was used to terminate the staining reaction, and the seedlings were mounted on slides in 50 μ L Hoyer's solution (chloral hydrate:water:glycerol; 8:3:1; w/v/v) and examined by differential interference contrast microscopy.

Measurement of IAA Levels

Roots of 3-d-old etiolated seedlings grown on MS or ACC (10 μ M) or ACC (10 μ M) plus Kyn (1.5 μ M) medium were used for endogenous IAA

measurement. These seedlings were pulled out of agar, arranged side-by-side on the surface of prewetted nylon filters resting on the surface of fresh MS or ACC (10 μ M) or ACC (10 μ M) plus Kyn (1.5 μ M) medium plates, dissected into roots and hypocotyls with a scalpel, and frozen in liquid nitrogen (Stepanova et al., 2008).

For analysis of IAA, the method is briefly described as the following: 100 mg plant tissue was homogenized and extracted for 24 h in methanol containing $^2\text{H}_2$ -IAA (purchased from CDN Isotopes) as internal standard. Purification was done with an Oasis Max solid phase extract cartridge (150 mg/6 cc; Waters) and eluted with 5% formic acid in methanol. The elution was dried with nitrogen gas and reconstituted in water/methanol (20:80, v/v) and finally was injected to a liquid chromatography–tandem mass spectrometry system consisting of an Acquity ultraperformance liquid chromatograph (Acquity UPLC; Waters) and a triple quadrupole tandem mass spectrometer (Quattro Premier XE; Waters) (Zhou et al., 2010). For the IAA quantification, we extracted the plant tissues using methanol at -20°C . The UPLC flow rate was set to 200 $\mu\text{L}/\text{min}$ with the mobile phase containing 0.05% acetic acid and the mass spectrometer source temperature set to 110°C . The step of eluting IAA from the MAX SPE column took ~ 10 min with the solvent containing 5% formic acid.

Computational Docking and Molecular Modeling

We used the AutoDock4 docking software (Huey et al., 2004) to model the interaction specificity between the small compounds and their target proteins, L-Kyn (ZINC ID:895186), L-Trp (ZINC ID:83315), KAT1 (PDB ID: 1W7L), and TAA1 (PDB ID: 3BWN), using the following steps: We first prepared compound/target files for subsequent rigid target-flexible compound docking by adding charged and polar hydrogen atoms. To speed up the interaction energy calculation, the subprogram AutoGrid was used to calculate the grid interaction energy between the probe of the compound atom type and the target. Then, the Lamarckian genetic algorithm–enhanced sampling method was used to obtain the poses of the target–compound complex. Those poses that contain protein clashes were removed. According to scoring, binding energy, and chemical reasonableness, we screened the results and obtained acceptable poses. Total compound–target interaction energy (kcal/mol) was predicted by the PEARLS program (Han et al., 2006), whereas protein flexibility was ignored in this work. Multiple factors, such as Van der Waals interaction, electrostatic interaction, hydrogen bond, solvation, and conformational entropy, were taken into account when calculating compound–target interaction energy.

Structure Alignment

Based on the three-dimensional structural similarity, the structure alignment was done using the program Pymol (<http://www.pymol.org>). The structure analysis of proteins provides information about the common alignment core.

For details on the phylogenetic analysis of the protein sequences, see Supplemental Methods 1 and Supplemental References 1 online.

Confocal Laser Microscopy

Zeiss LSM-710 with $\times 20$ and $\times 40$ objectives were used to detect GFP fluorescence. All seedlings were grown on MS medium in the dark for 3 d and then placed into liquid MS medium supplemented with the indicated chemicals (100 μM Kyn, 100 μM ACC, and 10 μM IAA) and incubated for 3 to 4 h in the dark. The seedlings were mounted on glass slides after chemical treatments and observed using a Zeiss LSM-710 microscope.

TAA1 Activity Assays

The TAA1 open reading frame was subcloned into pENTR/D-Topo and transferred into pDEST15 by Gateway LR recombination (Invitrogen) as

previously described (Stepanova et al., 2008). GST-TAA1 was expressed in the BL21 Star (DE3) pLysS strain of *Escherichia coli* (Invitrogen) and induced by 0.5 mM isopropyl β -D-1-thiogalactopyranoside for 4 h. Equal volumes of protein extracts were loaded onto a native 10% polyacrylamide gel and run for 2 h at 100 V at 4°C . The in-gel aminotransferase activity was assayed as described (Pedraza et al., 2004) at 24°C overnight. Biochemical characterization of TAA1 was performed using recombinant GST-TAA1 batch purified on glutathione-sepharose beads (Amersham Pharmacia) according to the manufacturer's recommendations. Purified protein concentrations were estimated by SDS-PAGE followed by Coomassie Brilliant Blue staining. For a 100- μL reaction, 5 μg of TAA1 was used. The reaction was performed at 55°C for 10 min using conditions as described (Koshiba and Matsuyama, 1993). K_m and V_{max} were determined by Graphpad Prism 5 software using nonlinear regression for the Michaelis-Menten equation with robust fit. Enzymatic activity of the purified GST-TAA1 was determined by HPLC as previously described (Stepanova et al., 2008).

Statistics

The values we obtained in the figures were expressed as the mean (\pm SD). Two-tailed Student's *t* tests were used ($P < 0.001$).

Accession Numbers

Sequence data from this article can be found in the Arabidopsis Genome Initiative or GenBank/EMBL databases under the following accession numbers: TAA1 (AT1g70560), TAR1 (AT1G23320), TAR2 (AT4G24670), TAR3 (AT1G34040), TAR4 (AT1G34060), WEI2 (AT5G05730), WEI7 (AT1G25220), EIN3 (AT3g20770), CTR1 (AT5g03730), and ETO1 (AT3g51770). Accession numbers of protein and chemicals structures used in the computational docking in Figure 7 are as follows: KAT1 (PDB ID: 1W7L), TAA1 (PDB ID: 3BWN), L-Kyn (ZINC ID:895186), and L-Trp (ZINC ID:83315). Accession numbers for the sequences used in the multiple sequence alignment in Figure 7F are in that figure, and accession numbers for the sequences used in the phylogenetic analysis are on the tree in Supplemental Figure 8 and Supplemental Data Set 1 online.

Supplemental Data

The following materials are available in the online version of this article.

Supplemental Figure 1. Kyn Effectively Promotes Root Elongation in a Concentration-Dependent Manner.

Supplemental Figure 2. Kyn Inhibits Ethylene-Induced Root Hair Formation as Well as *EBS:GUS* Expression in Roots.

Supplemental Figure 3. High Concentrations of Kyn Could Induce Hook Opening Phenotypes of 3-d-Old Etiolated Seedlings.

Supplemental Figure 4. Kyn Has Minimal Effects on Ethylene-Insensitive Mutants.

Supplemental Figure 5. Kyn Does Not Interfere with Jasmonic Acid, Cytokinin, and ABA Signaling Pathways.

Supplemental Figure 6. Kyn, but Not Its Metabolites, Inhibits TAA1.

Supplemental Figure 7. High Doses of Exogenous Trp Block the Stimulating Effect of Kyn on Root Elongation.

Supplemental Figure 8. Phylogenetic Tree and Sequence Alignments of Annotated Aminotransferases in *Arabidopsis*.

Supplemental Figure 9. Kyn Has No Effect on *E. coli*-derived Aminotransferase.

Supplemental Figure 10. IAA Stabilizes EIN3-GFP but Does Not Alter the Stability of EBF1-GFP or GFP-EBF2.

Supplemental Table 1. The Free Energy of Binding for the Interactions of KAT1 and Kyn, TAA1 and Kyn, and TAA1 and Trp Are Similar.

Supplemental Methods 1. Phylogenetic Analysis.

Supplemental References 1. Supplemental References for Supplemental Methods 1.

Supplemental Data Set 1. Text File of the Alignment Used to Generate the Tree in Supplemental Figure 8A.

ACKNOWLEDGMENTS

We thank Yuxuan Pang (Tsinghua University), Ziqiang Zhu, and Wen Wan (Peking University) for critical reading of the manuscript. We thank Dao-Xin Xie (Tsinghua University) for providing the *Thi2.1::GUS* seeds. This work was supported by grants from the National Natural Science Foundation of China (30730011 and 91017010) and the Ministry of Agriculture of China (2010ZX08010-002) to H.G., by the National Science Foundation (Grants DBI0820755 and MCB0923727) to J.M.A. and A.N.S., by the U.S. National Institute of General Sciences (Grants GM081451 and GM081451-03S2) to Z.Y., and by a U.S. National Science Foundation Integrative Graduate Education and Research Traineeship Program Grant (DGE0504249) for the compound libraries. H.L. was also supported in part by the China Scholarship Council, and J.B. was supported in part by Ministerio de Educacion, Programa Nacional de Movilidad de Recursos Humanos del Plan Nacional de I-D+i 2008-2011. The publication fee is covered by the 111 Project of Peking University.

AUTHOR CONTRIBUTIONS

H.G., W.H., and H.L. conceived the project and designed the experiments. W.H. performed and analyzed most of the phenotypes, performed GUS staining and GFP fluorescence detection, and conjectured the target of Kyn. H.L., N.R., and Z.Y. conducted the chemical library screens and the initial characterization of small molecule candidates. J.B., A.N.S., J.M.A., and D.-Y.X. tested the TAA1 activity in vitro. A.N.S. performed the L-Kyn sensitivity assays in *wei8* and *TAA1::GFP-TAA1*. Y.J. constructed the phylogenetic tree, tested statistics, and coordinated the figures. M.K. and N.Y. did the molecular docking and structure alignment, and X.G. calculated the free energy of binding. Q.Z. helped measure root length phenotypes. W.L., X.Z., X.W., and F.A. did most of the genetic crosses in this article. J.C., X.S., and C.Y. measured IAA levels. W.H., P.L., and H.G. wrote the article. All authors analyzed and discussed the data and the article.

Received July 11, 2011; revised October 8, 2011; accepted October 26, 2011; published November 22, 2011.

REFERENCES

- Abel, S., Nguyen, M.D., Chow, W., and Theologis, A. (1995). ACS4, a primary indoleacetic acid-responsive gene encoding 1-aminocyclopropane-1-carboxylate synthase in *Arabidopsis thaliana*. Structural characterization, expression in *Escherichia coli*, and expression characteristics in response to auxin [corrected]. *J. Biol. Chem.* **270**: 19093–19099. Erratum. *J. Biol. Chem.* **270**: 26020.
- Alonso, J.M., Hirayama, T., Roman, G., Nourizadeh, S., and Ecker, J.R. (1999). EIN2, a bifunctional transducer of ethylene and stress responses in *Arabidopsis*. *Science* **284**: 2148–2152.
- Alonso, J.M., Stepanova, A.N., Solano, R., Wisman, E., Ferrari, S., Ausubel, F.M., and Ecker, J.R. (2003). Five components of the ethylene-response pathway identified in a screen for weak ethylene-insensitive mutants in *Arabidopsis*. *Proc. Natl. Acad. Sci. USA* **100**: 2992–2997.
- An, F., et al. (2010). Ethylene-induced stabilization of ETHYLENE INSENSITIVE3 and EIN3-LIKE1 is mediated by proteasomal degradation of EIN3 binding F-box 1 and 2 that requires EIN2 in *Arabidopsis*. *Plant Cell* **22**: 2384–2401.
- Armstrong, J.I., Yuan, S., Dale, J.M., Tanner, V.N., and Theologis, A. (2004). Identification of inhibitors of auxin transcriptional activation by means of chemical genetics in *Arabidopsis*. *Proc. Natl. Acad. Sci. USA* **101**: 14978–14983.
- Beadle, G.W., Mitchell, H.K., and Nyc, J.F. (1947). Kynurenine as an intermediate in the formation of nicotinic acid from tryptophan by *Neurospora*. *Proc. Natl. Acad. Sci. USA* **33**: 155–158.
- Benjamins, R., and Scheres, B. (2008). Auxin: The looping star in plant development. *Annu. Rev. Plant Biol.* **59**: 443–465.
- Bennett, M.J., Marchant, A., Green, H.G., May, S.T., Ward, S.P., Millner, P.A., Walker, A.R., Schulz, B., and Feldmann, K.A. (1996). *Arabidopsis* AUX1 gene: A permease-like regulator of root gravitropism. *Science* **273**: 948–950.
- Bleecker, A.B., and Kende, H. (2000). Ethylene: A gaseous signal molecule in plants. *Annu. Rev. Cell Dev. Biol.* **16**: 1–18.
- Boller, T., Herner, R.C., and Kende, H. (1979). Assay for and enzymatic formation of an ethylene precursor, 1-aminocyclopropane-1-carboxylic acid. *Planta* **145**: 293–303.
- Campesan, S., Green, E.W., Breda, C., Sathyaikumar, K.V., Muchowski, P.J., Schwarcz, R., Kyriacou, C.P., and Giorgini, F. (2011). The kynurenine pathway modulates neurodegeneration in a *Drosophila* model of Huntington's disease. *Curr. Biol.* **21**: 961–966.
- Cerqueira, N.M.F.S.A., Fernandes, P.A., and Ramos, M.J. (2011). Computational mechanistic studies addressed to the transamination reaction present in all pyridoxal 5'-phosphate-requiring enzymes. *J. Chem. Theory Comput.* **7**: 1356–1368.
- Chao, Q., Rothenberg, M., Solano, R., Roman, G., Terzaghi, W., and Ecker, J.R. (1997). Activation of the ethylene gas response pathway in *Arabidopsis* by the nuclear protein ETHYLENE-INSENSITIVE3 and related proteins. *Cell* **89**: 1133–1144.
- Crews, C.M., and Splittergerber, U. (1999). Chemical genetics: Exploring and controlling cellular processes with chemical probes. *Trends Biochem. Sci.* **24**: 317–320.
- D'Agostino, I.B., Deruère, J., and Kieber, J.J. (2000). Characterization of the response of the *Arabidopsis* response regulator gene family to cytokinin. *Plant Physiol.* **124**: 1706–1717.
- De Rybel, B., Audenaert, D., Beeckman, T., and Kepinski, S. (2009a). The past, present, and future of chemical biology in auxin research. *ACS Chem. Biol.* **4**: 987–998.
- De Rybel, B., et al. (2009b). Chemical inhibition of a subset of *Arabidopsis thaliana* GSK3-like kinases activates brassinosteroid signaling. *Chem. Biol.* **16**: 594–604.
- Epple, P., Apel, K., and Bohmann, H. (1995). An *Arabidopsis thaliana* thionin gene is inducible via a signal transduction pathway different from that for pathogenesis-related proteins. *Plant Physiol.* **109**: 813–820.
- Foster, A.C., Vezzani, A., French, E.D., and Schwarcz, R. (1984). Kynurenic acid blocks neurotoxicity and seizures induced in rats by the related brain metabolite quinolinic acid. *Neurosci. Lett.* **48**: 273–278.
- Gagne, J.M., Smalle, J., Gingerich, D.J., Walker, J.M., Yoo, S.D., Yanagisawa, S., and Vierstra, R.D. (2004). *Arabidopsis* EIN3-binding F-box 1 and 2 form ubiquitin-protein ligases that repress ethylene

- action and promote growth by directing EIN3 degradation. *Proc. Natl. Acad. Sci. USA* **101**: 6803–6808.
- Girke, T., Cheng, L.C., and Raikhel, N.** (2005). ChemMine. A compound mining database for chemical genomics. *Plant Physiol.* **138**: 573–577.
- Guo, H., and Ecker, J.R.** (2003). Plant responses to ethylene gas are mediated by SCF(EBF1/EBF2)-dependent proteolysis of EIN3 transcription factor. *Cell* **115**: 667–677.
- Guzmán, P., and Ecker, J.R.** (1990). Exploiting the triple response of *Arabidopsis* to identify ethylene-related mutants. *Plant Cell* **2**: 513–523.
- Han, L.Y., Lin, H.H., Li, Z.R., Zheng, C.J., Cao, Z.W., Xie, B., and Chen, Y.Z.** (2006). PEARLS: Program for energetic analysis of receptor-ligand system. *J. Chem. Inf. Model.* **46**: 445–450.
- Han, Q., Robinson, H., Cai, T., Tagle, D.A., and Li, J.** (2009). Structural insight into the inhibition of human kynurenine aminotransferase I/glutamine transaminase K. *J. Med. Chem.* **52**: 2786–2793.
- Huai, Q., Xia, Y., Chen, Y., Callahan, B., Li, N., and Ke, H.** (2001). Crystal structures of 1-aminocyclopropane-1-carboxylate (ACC) synthase in complex with aminoethoxyvinylglycine and pyridoxal-5'-phosphate provide new insight into catalytic mechanisms. *J. Biol. Chem.* **276**: 38210–38216.
- Huey, R., Goodsell, D.S., Morris, G.M., and Olson, A.J.** (2004). Grid-based hydrogen bond potentials with improved directionality. *Lett. Drug Des. Discov.* **1**: 178–183.
- Ilić, N., Östin, A., and Cohen, J.D.** (1999). Differential inhibition of indole-3-acetic acid and tryptophan biosynthesis by indole analogues. I. Tryptophan dependent IAA biosynthesis. *Plant Growth Regul.* **27**: 57–62.
- Johnson, P.R., and Ecker, J.R.** (1998). The ethylene gas signal transduction pathway: A molecular perspective. *Annu. Rev. Genet.* **32**: 227–254.
- Jönsson, H., Heisler, M.G., Shapiro, B.E., Meyerowitz, E.M., and Mjolsness, E.** (2006). An auxin-driven polarized transport model for phyllotaxis. *Proc. Natl. Acad. Sci. USA* **103**: 1633–1638.
- Katoh, A., and Hashimoto, T.** (2004). Molecular biology of pyridine nucleotide and nicotine biosynthesis. *Front. Biosci.* **9**: 1577–1586.
- Kieber, J.J., Rothenberg, M., Roman, G., Feldmann, K.A., and Ecker, J.R.** (1993). CTR1, a negative regulator of the ethylene response pathway in *Arabidopsis*, encodes a member of the raf family of protein kinases. *Cell* **72**: 427–441.
- Koshiba, T., and Matsuyama, H.** (1993). An in vitro system of indole-3-acetic acid formation from tryptophan in maize (*Zea mays*) coleoptile extracts. *Plant Physiol.* **102**: 1319–1324.
- Koshiba, T., Mito, N., and Miyakado, M.** (1993). L-tryptophan and D-tryptophan aminotransferases from maize coleoptiles. *J. Plant Res.* **106**: 25–29.
- Ludwig-Müller, J., Denk, K., Cohen, J.D., and Quint, M.** (2010). An inhibitor of tryptophan-dependent biosynthesis of indole-3-acetic acid alters seedling development in *Arabidopsis*. *J. Plant Growth Regul.* **29**: 242–248.
- Luschnig, C., Gaxiola, R.A., Grisafi, P., and Fink, G.R.** (1998). EIR1, a root-specific protein involved in auxin transport, is required for gravitropism in *Arabidopsis thaliana*. *Genes Dev.* **12**: 2175–2187.
- Müller, A., Guan, C., Gälweiler, L., Tänzler, P., Huijser, P., Marchant, A., Parry, G., Bennett, M., Wisman, E., and Palme, K.** (1998). AtPIN2 defines a locus of *Arabidopsis* for root gravitropism control. *EMBO J.* **17**: 6903–6911.
- Park, S.Y., et al.** (2009). Abscisic acid inhibits type 2C protein phosphatases via the PYR/PYL family of START proteins. *Science* **324**: 1068–1071.
- Pedraza, R.O., Ramírez-Mata, A., Xiqui, M.L., and Baca, B.E.** (2004). Aromatic amino acid aminotransferase activity and indole-3-acetic acid production by associative nitrogen-fixing bacteria. *FEMS Microbiol. Lett.* **233**: 15–21.
- Phillips, K.A., Skirpan, A.L., Liu, X., Christensen, A., Slewinski, T.L., Hudson, C., Barazesh, S., Cohen, J.D., Malcomber, S., and McSteen, P.** (2011). vanishing tassel2 encodes a grass-specific tryptophan aminotransferase required for vegetative and reproductive development in maize. *Plant Cell* **23**: 550–566.
- Potuschak, T., Lechner, E., Parmentier, Y., Yanagisawa, S., Grava, S., Koncz, C., and Genschik, P.** (2003). EIN3-dependent regulation of plant ethylene hormone signaling by two arabidopsis F box proteins: EBF1 and EBF2. *Cell* **115**: 679–689.
- Quaedvlieg, N.E., Schlaman, H.R., Admiraal, P.C., Wijting, S.E., Stougaard, J., and Spink, H.P.** (1998). Fusions between green fluorescent protein and beta-glucuronidase as sensitive and vital bifunctional reporters in plants. *Plant Mol. Biol.* **38**: 861–873.
- Reinhardt, D., Pesce, E.R., Stieger, P., Mandel, T., Baltensperger, K., Bennett, M., Traas, J., Friml, J., and Kuhlemeier, C.** (2003). Regulation of phyllotaxis by polar auxin transport. *Nature* **426**: 255–260.
- Růžička, K., Ljung, K., Vanneste, S., Podhorská, R., Beeckman, T., Friml, J., and Benková, E.** (2007). Ethylene regulates root growth through effects on auxin biosynthesis and transport-dependent auxin distribution. *Plant Cell* **19**: 2197–2212.
- Sas, K., Robotka, H., Toldi, J., and Vécsei, L.** (2007). Mitochondria, metabolic disturbances, oxidative stress and the kynurenine system, with focus on neurodegenerative disorders. *J. Neurol. Sci.* **257**: 221–239.
- Schwarcz, R., Whetsell, W.O., Jr., and Mangano, R.M.** (1983). Quinolinic acid: An endogenous metabolite that produces axon-sparing lesions in rat brain. *Science* **219**: 316–318.
- Smith, R.S., Guyomarc'h, S., Mandel, T., Reinhardt, D., Kuhlemeier, C., and Prusinkiewicz, P.** (2006). A plausible model of phyllotaxis. *Proc. Natl. Acad. Sci. USA* **103**: 1301–1306.
- Soeno, K., Goda, H., Ishii, T., Ogura, T., Tachikawa, T., Sasaki, E., Yoshida, S., Fujioka, S., Asami, T., and Shimada, Y.** (2010). Auxin biosynthesis inhibitors, identified by a genomics-based approach, provide insights into auxin biosynthesis. *Plant Cell Physiol.* **51**: 524–536.
- Stepanova, A.N., Hoyt, J.M., Hamilton, A.A., and Alonso, J.M.** (2005). A link between ethylene and auxin uncovered by the characterization of two root-specific ethylene-insensitive mutants in *Arabidopsis*. *Plant Cell* **17**: 2230–2242.
- Stepanova, A.N., Robertson-Hoyt, J., Yun, J., Benavente, L.M., Xie, D.Y., Dolezal, K., Schlereth, A., Jürgens, G., and Alonso, J.M.** (2008). TAA1-mediated auxin biosynthesis is essential for hormone crosstalk and plant development. *Cell* **133**: 177–191.
- Stepanova, A.N., Yun, J., Likhacheva, A.V., and Alonso, J.M.** (2007). Multilevel interactions between ethylene and auxin in *Arabidopsis* roots. *Plant Cell* **19**: 2169–2185.
- Swarup, R., Perry, P., Hagenbeek, D., Van Der Straeten, D., Beemster, G.T., Sandberg, G., Bhalerao, R., Ljung, K., and Bennett, M.J.** (2007). Ethylene upregulates auxin biosynthesis in *Arabidopsis* seedlings to enhance inhibition of root cell elongation. *Plant Cell* **19**: 2186–2196.
- Tao, Y., et al.** (2008). Rapid synthesis of auxin via a new tryptophan-dependent pathway is required for shade avoidance in plants. *Cell* **133**: 164–176.
- Tóth, R., and van der Hoorn, R.A.** (2010). Emerging principles in plant chemical genetics. *Trends Plant Sci.* **15**: 81–88.
- Tsuchisaka, A., and Theologis, A.** (2004). Unique and overlapping expression patterns among the *Arabidopsis* 1-amino-cyclopropane-1-carboxylate synthase gene family members. *Plant Physiol.* **136**: 2982–3000.

- Tsurusaki, K., Watanabe, S., Sakurai, N., and Kuraishi, S.** (1990). Conversion of D-tryptophan to indole-3-acetic-acid in coleoptiles of a normal and a semidwarf barley (*Hordeum vulgare*) strain. *Physiol. Plant.* **79**: 221–225.
- Wang, K.L., Yoshida, H., Lurin, C., and Ecker, J.R.** (2004). Regulation of ethylene gas biosynthesis by the Arabidopsis ETO1 protein. *Nature* **428**: 945–950.
- Xu, T., Wen, M., Nagawa, S., Fu, Y., Chen, J.G., Wu, M.J., Perrot-Rechenmann, C., Friml, J., Jones, A.M., and Yang, Z.** (2010). Cell surface- and rho GTPase-based auxin signaling controls cellular interdigitation in Arabidopsis. *Cell* **143**: 99–110.
- Yamada, M., Greenham, K., Prigge, M.J., Jensen, P.J., and Estelle, M.** (2009). The TRANSPORT INHIBITOR RESPONSE2 gene is required for auxin synthesis and diverse aspects of plant development. *Plant Physiol.* **151**: 168–179.
- Zhao, Y.** (2010). Auxin biosynthesis and its role in plant development. *Annu. Rev. Plant Biol.* **61**: 49–64.
- Zhou, W., Wei, L., Xu, J., Zhai, Q., Jiang, H., Chen, R., Chen, Q., Sun, J., Chu, J., Zhu, L., Liu, C.M., and Li, C.** (2010). Arabidopsis tyrosylprotein sulfotransferase acts in the auxin/PLETHORA pathway in regulating postembryonic maintenance of the root stem cell niche. *Plant Cell* **22**: 3692–3709.
- Zwilling, D., et al.** (2011). Kynurenine 3-monooxygenase inhibition in blood ameliorates neurodegeneration. *Cell* **145**: 863–874.